synthetic intermediates in the preparation of other nitrite-containing complexes, e.g. five-coordinate or mixed-axial-ligand species, is under active investigation.

Contribution from the Department of Chemistry,
The University of Michigan, Ann Arbor, Michigan 48109

Binucleating Macrocyclic [14]N4 Ligands and Their Complexes. Synthesis of the Free Ligand 2,3-Dioxo-5,6:13,14-dibenzo-9,10-(4',5'-dimethylbenzo)-1,4,8,11-tetraazacyclotetradeca-7,11-diene (L) and of the 7,12-Me2-L Metal Complexes and Derivatives. Crystal Structures and Properties of the [M'][M(7,12-Me2-L)] Complexes (M = Ni(II); M = Co(II); M' = ZnCl2, M = Ni(II); M' = [Na(5-crown-15)]+, M = Ni(II); M' = [(C2H5)4N]+, M = Ni(II))

D. Christodoulou, M. G. Kanatzidis, and D. Coucouvanis*

The free macrocyclic ligand 2,3-dioxo-5,6:13,14-dibenzo-9,10-(4',5'-dimethylbenzo)-1,4,8,11-tetraazacyclotetradeca-7,11-diene, abbreviated α-diketo-TAD-Me2, and its complexes with Ni(II) and Co(II) have been synthesized. The Ni(II) complex readily undergoes reduction and by virtue of the α-diketone function, appended to the macrocyclic ring, can bind to other metal ions. Complexes of the 2,3-dioxo-5,6:13,14-dibenzo-7,12-dimethyl-9,10-(4',5'-dimethylbenzo)-1,4,8,11-tetraazacyclotetradeca-7,11-diene, abbreviated α-diketo-TAD-Me4, also have been synthesized. The structures of Ni(α-diketo-TAD-Me4) (IVa), of the reduction derivatives (Et4N)[Ni(α-diketo-TAD-Me4+H)] (V) and [Na(5-crown-15)][Ni(α-diketo-TAD-Me4+H)] (VI), and of the binuclear complex [Ni(α-diketo-TAD-Me4)]ZnCl2 (VII) are reported. Crystals of IVa are orthorhombic, space group *Pnam*; a = 7.934 (4) Å, b = 12.663 (6) Å, and c = 20.922 (9) Å. Crystals of V are monoclinic, space group *P2₁/a*; a = 14.789 (6) Å, b = 17.582 (5) Å, c = 15.372 (6) Å, and β = 108.36 (3)°. Crystals of VI are monoclinic, space group *P2₁/n*; a = 17.201 (11) Å, b = 12.113 (11) Å, c = 17.426 (12) Å, and β = 75.32 (5)°. Crystals of VII are monoclinic, space group *P2₁/c*; a = 11.139 (9) Å, b = 16.19 (2) Å, c = 16.15 (1) Å, and β = 98.03 (7)°. Refinements by full-matrix least squares of 151 parameters on 1085 data for IVa, of 371 parameters on 2455 data for V, of 349 parameters on 2440 data for VI, and of 215 parameters on 1514 data for VII converged to the *R* values of 0.044, 0.073, 0.078, and 0.073, respectively. In all structures the hydrogen atoms were included in the structure factor calculations but were not refined. In IVa the macrocycle adopts a saddle-shaped conformation and the molecules stack along the crystallographic *a* axis. The planar NiN4 chromophores are equally spaced with a Ni–Ni distance of 4.059 (1) Å. In V and VI the reduction has resulted in the saturation of one of the imino bonds, and in the structure of VI the Na+ ion is coordinated by the α-diketo function and is found at 5.070 (9) Å from the Ni atom. In VII the Zn atom also is coordinated by the α-diketo function and is located 5.140 (3) Å from the Ni atom. The electrochemistry and electronic spectra of the complexes are reported. Co(α-diketo-TAD-Me2), which is a high-spin, square-planar Co(II) complex, shows a quasireversible reduction at −0.86 V vs SCE and binds O2 reversibly.

Introduction

A rapidly emerging area of chemical interest in recent years concerns the synthesis of heterobinucleating ligands and the coordination chemistry of the heteronuclear complexes that derive from such ligands. Examples of heterobinucleating ligands that could serve as "polytopic receptor molecules"[1] for the binding of metal cations, or the cobinding of metal ions and molecular substrates, include molecules that contain macrocyclic (polyether) functionalities appended to porphyrin[1] or *N,N'*-ethylenebis(salicylideneaminato)[2] (salen) centers, phenols appended to macrocyclic tetraamines,[3] and aromatic phosphines appended to the acetylacetonate anion.[4]

In addition to the employment of specifically designed ligand systems as mentioned above, heterometallic complexes have been obtained also in reactions where metal complexes are used as

ligands for various Lewis acids. In these reactions, the availability of more than one lone pair on a donor atom, or of multiple donor atoms within a coordinated ligand, introduce the potential for second-order interactions that under appropriate conditions lead to heteronuclear aggregates. Included in this class are complexes derived from metal cyanides,[5] metal thiocyanates,[6] (η^5-C5H5)2M-(SR)2 complexes (M = Ti,[7] Mo,[8] W,[8] Nb[9]), (η^5-C5H5)2Zr(PPh2)2 complexes,[10] salen complexes,[11,12] the tetrathiometalate anions,

(1) Hamilton, A.; Lehn, J. M.; Sessler, J. L. *J. Am. Chem. Soc.* **1986,** *108*, 5158–5167.

(2) van Staveren, C. J.; Reinhoudt, D. N.; van Eerden, J.; Harkema, S. *J. Chem. Soc., Chem. Commun.* **1987,** 974–977.

(3) Kimura, E.; Koike, T.; Uenishi, K.; Hediger, M.; Kuramoto, M.; Joko, S.; Arai, Y.; Kodama, M.; Iitaka, Y. *Inorg. Chem.* **1987,** *26*, 2975–2983.

(4) Wrobleski, D.; Rauchfuss, T. B. *J. Am. Chem. Soc.* **1982,** *104*, 2314–2316.

(5) Ludi, A.; Gudel, H. U. *Struct. Bonding* **1973,** *14*, 1.

(6) Armor, J. N.; Haim, A. *J. Am. Chem. Soc.* **1971,** *93*, 867.

(7) (a) Braterman, P. S.; Wilson, V. A. *J. Organomet. Chem.* **1971,** *31*, 131. (b) Braterman, P. S.; Wilson, V. A.; Joshi, K. K. *J. Organomet. Chem.* **1971,** *31*, 123. (c) Dias, A. R.; Green, M. L. H. *Rev. Port. Quim.* **1969,** *11*, 61.

(8) Dias, A. R.; Green, M. L. H. *J. Chem. Soc. A* **1971,** 1951.

(9) Douglas, W. E.; Green, M. L. H. *J. Chem. Soc., Dalton Trans.* **1972,** 1796.

(10) (a) Gelmini, L.; Stephan, D. W. *Inorg. Chem.* **1986,** *25*, 1222–1225. (b) Gelmini, L.; Matassa, L. C.; Stephan, D. W. *Inorg. Chem.* **1985,** *24*, 2585–2588.

(11) (a) Sinn, E.; Harris, C. M. *Coord. Chem. Rev.* **1969,** *4*, 391. (b) Hobday, M. D.; Smith, T. D. *Ibid.* **1972,** *9*, 311. (c) Bear, C. A.; Waters, J. M.; Waters, T. N. *J. Chem. Soc., Dalton Trans.* **1974,** 1059. (d) Gruber, S. J.; Harris, C. M.; Sinn, E. *J. Inorg. Nucl. Chem.* **1968,** *30*, 1805.

Scheme I

Ia, R=H
Ib, R=Me

IIa, R=H
IIb, R=Me

III. R=H

α-diketo-TAD-Me₂
III

M=Ni, Co
R=H
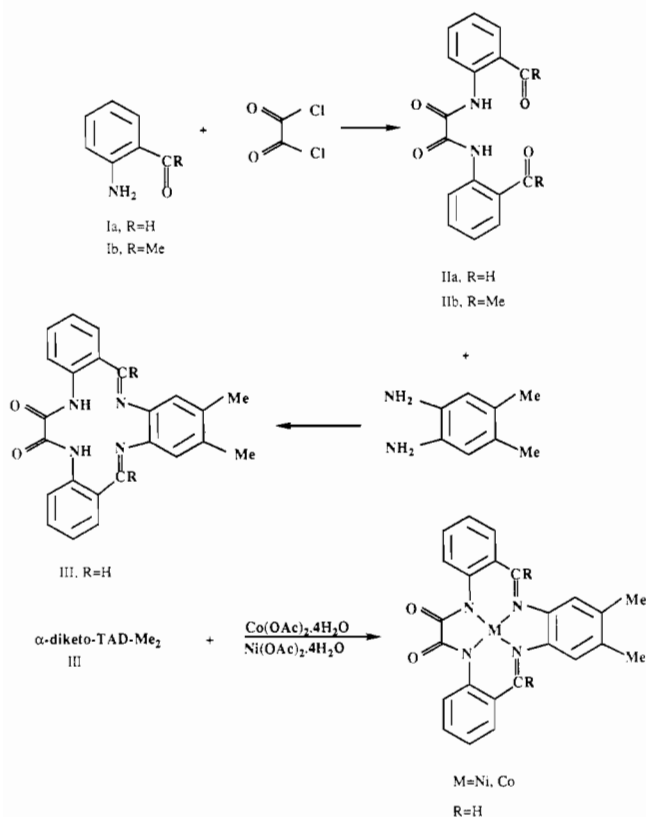
$[MS_4]^{n-}$ (M = Mo, W, n = 2;[13,14] M = V,[15] n = 1; M = Re, n = 3[16]), and the metal dithiooxalato complexes.[17]

The organization of metal ions with diverse electronic properties within a template ligand system potentially can lead to the appropriate orientation and/or polarization of substrate molecules necessary for particular reactions. In an elementary sense, such systems may mimic features of certain metalloenzymes, where precise orientation and activation of substrate molecules lead to the efficient catalysis of specific reactions.

We report herein the synthesis of the free macrocyclic ligand 2,3-dioxo-5,6:13,14-dibenzo-9,10-(4',5'-dimethylbenzo)-1,4,8,11-tetraazacyclotetradeca-7,11-diene (Scheme I; III), abbreviated as α-diketo-TAD-Me₂, and the synthesis, properties, and reactivity of the Ni(II) and Co(II) complexes of this ligand. The synthesis of complexes with the 2,3-dioxo-5,6:13,14-dibenzo-7,12-dimethyl-9,10-(4',5'-dimethylbenzo)-1,4,8,11-tetraazacyclotetradeca-7,11-diene ligand, abbreviated as α-diketo-TAD-Me₄ also is reported. The structures of Ni(α-diketo-TAD-Me₄), of the reduction derivatives [Na(5-crown-15)][Ni(α-diketo-TAD-Me₄+H)] and (Et₄N)[Ni(α-diketo-TAD-Me₄+H)], and of the binuclear [Ni(α-diketo-TAD-Me₄)]ZnCl₂ complex have been determined. The synthesis of the M(α-diketo-TAD-Me₄) complexes (M = Ni, Co) has been reported previously.[18]

(12) (a) Gambarotta, S.; Arena, F.; Floriani, C.; Zanazzi, P. F. *J. Am. Chem. Soc.* **1982**, *104*, 5082–5092. (b) Pasquali, M.; Marchetti, F.; Floriani, C.; Cesari, M. *Inorg. Chem.* **1980**, *19*, 1198–1202. (c) Gambarotta, S.; Urso, F.; Floriani, C.; Chiesi-Villa, A.; Guastini, C. *Inorg. Chem.* **1983**, *22*, 3966–3972. (d) Gambarotta, S.; Corazza, F.; Floriani, C.; Zehnder, M. *J. Chem. Soc., Chem. Commun.* **1984**, 1305–1307.
(13) Diemann, E.; Muller, A. *Coord. Chem. Rev.* **1973**, *10*, 79.
(14) Coucouvanis, D. *Acc. Chem. Res.* **1981**, *14*, 201.
(15) Do, Y.; Simhon, E. D.; Holm, R. H. *Inorg. Chem.* **1985**, *24*, 4635.
(16) (a) Muller, A.; Krickemeyer, E.; Bogge, H. *Z. Anorg. Allg. Chem.* **1987**, *554*, 61–78. (b) Cotton, F. A.; Kibala, P. A.; Matusc, M. *Polyhedron* **1988**, *7*, 83.
(17) (a) Coucouvanis, D.; Baenziger, N. C.; Johnson, S. M. *J. Am. Chem. Soc.* **1973**, *95*, 3875. (b) Coucouvanis, D.; Piltingsrud, D. *J. Am. Chem. Soc.* **1973**, *95*, 5556. (c) Coucouvanis, D. *Transition Metal Chemistry, Current Problems of General Biological and Catalytic Relevance*; Muller, A., Diemann, E., Eds.; Verlag Chemie: Weinheim, West Germany, 1981; p 59–89.

Experimental Section

The chemicals in this research were used as purchased. The *o*-phenylenediamine and 4,5-dimethyl-*o*-phenylenediamine were purchased from Aldrich Chemical Co., stored under N₂, and recrystallized from hot benzene prior to use. The *o*-aminoacetophenone was also purchased from Aldrich Chemical Co., and the *o*-aminobenzaldehyde, from Fluka and stored at −20 °C. Dimethylformamide, DMF, was stored over 4A Linde molecular sieves over a period of 2 days and then distilled under reduced pressure at 30 °C. Acetone was dried over 4A Linde molecular sieves and then distilled. Diethyl ether and dichloromethane, CH₂Cl₂, were distilled from calcium hydride before use, and tetrahydrofuran, THF, was distilled over sodium benzophenone. Elemental analyses on samples, dried under vacuum for 6 h, were performed by Galbraith Analytical Laboratories, Knoxville, TN.

Visible and ultraviolet spectra were recorded on a Varian Cary Model 219 spectrophotometer. Infrared spectra were recorded on a Nicolet 60-DX FT-IR spectrophotometer. Proton NMR spectra were recorded on a Bruker FX 300-MHz pulse FT-NMR spectrometer with Me₄Si as internal standard. Chemical shifts are reported as parts per million (ppm). Magnetic susceptibility measurements with the Evans NMR method were carried out on the same instrument or a JEOL FX90Q pulse FT-NMR spectrometer. Magnetic susceptibility measurements on solid samples were performed with either a Johnson-Mathey balance or a SQUID magnetometer.

Electrochemical measurements were performed with a PAR Model 173 potentiostat/galvanostat and a PAR Model 175 universal programmer. The electrochemical cell used had platinum working and auxiliary electrodes. As a reference electrode, a saturated calomel electrode was used. The electrochemical measurements were performed in 0.1 M solutions in tetra-*n*-butylammonium perchlorate, *n*-Bu₄NClO₄, and were ~0.002 M in electroanalyte. Purified argon was used to purge these solutions prior to all measurements. The powder diffraction diagrams were obtained by using a 114 nm diameter Debye–Scherrer type camera with Ni-filtered Cu Kα radiation (λ = 1.541 8 Å).

Syntheses. 2,3-Dioxo-5,6:13,14-dibenzo-9,10-(4',5'-dimethylbenzo)-1,4,8,11-tetraazacyclotetradeca-7,11-diene, α-diketo-TAD-Me₂ (Scheme I; III). The yellow macrocyclic ligand was prepared by a Schiff-base condensation of the ligand precursor 2,2'-(oxalyldiimino)bis(benzaldehyde) (Scheme I, IIa) with 4,5-dimethyl-*o*-phenylenediamine. The ligand precursor (IIa) was prepared from *o*-aminobenzaldehyde and oxalyl chloride according to Armarego and Wilette[19] in a maximum yield of 40%.

IIa (2.02 g, 6.8 mmol) was heated in 650 mL of distilled DMF until completely dissolved, and to this solution was added a solution of 0.93 g (6.8 mmol) 4,5-dimethyl-*o*-phenylenediamine in 20 mL of DMF. The solution was heated at 110 °C under N₂ for a total of 60 h. The orange-yellow solution was ice-cooled, and ice-cold water, about 400 mL, was added in small portions to precipitate out the ligand. The ligand was filtered out, dried overnight in a vacuum desiccator over CaCl₂, and used for further synthesis without purification. It can be recrystallized from a hot dichloroethane/petroleum ether solution. Yield: 2.53 g; 93%. The compound does not show a melting point and decomposes above 200 °C.

Anal. Calcd for C₂₄H₂₀N₄O₂ (mol wt 396): C, 72.72; H, 5.05; N, 14.14. Found: C, 69.83; H, 5.05, N, 13.49.

The FAB mass spectrum in the matrix triethylenetetramine shows the molecular ion peak increased by a molecule of the matrix as an anion, (M − H⁺ + matrix)⁻ (*m/e* = 541), by negative ion scan. The monomer (M − H⁺ + 2matrix)⁻ (*m/e* 687) and dimer (M₂ + 2H)⁻ (*m/e* = 794) and (M₂ + matrix)⁻ (*m/e* = 938) ions are also present. The positive ion scan in the same matrix shows as the highest intensity mass peak (M + H⁺ + matrix)⁺ (*m/e* = 543).

FT-IR (cm⁻¹): 3022 (v), 2970 (w) 2946 (w), 2919 (w), 1696 (s), 1619 (s), 1608 (s), 1580 (s), 1512 (vs), 1446 (s), 1372 (m), 1359 (m) 1314 (m), 1295 (m), 1314 (m), 1295 (m), 1163 (m), 864 (m), 755 (s), 557 (w), 496 (w).

¹H NMR in DMSO-*d₆* (ppm): 10.05 (d, −NH), 8.76 (m, arom or HC=N), 8.15 (d, arom), 8.05 (arom), 7.79 (t, arom) 7.6 (m, arom), 7.45 (t, arom), 7.37 (t, arom), 7.2 (m, arom), 7.08 (m, arom), 6.78 (t, arom), 2.34 (d, −Me). The aromatic (arom) and HC=N protons overlap in the region δ 6.5–8.8. The ratio of aromatic to methyl protons is 12:6 (10 aromatic protons including 2 HC=N protons).

The Schiff-base condensation employed for the synthesis of ligand III (Scheme I) does not proceed for the ligand precursor 2,2'-(oxalyldiimino)bis(acetophenone) (Scheme I; IIb, R = Me).

(18) (a) Black, D. St. C.; Bos Vanderzalm, C. H.; Wong, L. C. H. *Aust. J. Chem.* **1982**, *35*, 2435–43. (b) Black, D. St. C.; Moss, G. I. *Aust. J. Chem.* **1987**, *40*, 129–142.
(19) Armarego, W. L. F.; Wilette, R. E. *J. Chem. Soc.* **1965**, 1258.

Scheme II

IIa, R=H
IIb, R=Me

IVa, R=Me, R'=Me
IVb, R=Me, R'=H
IVc, R=H, R'=Me
IVd, R=H, R'=Me
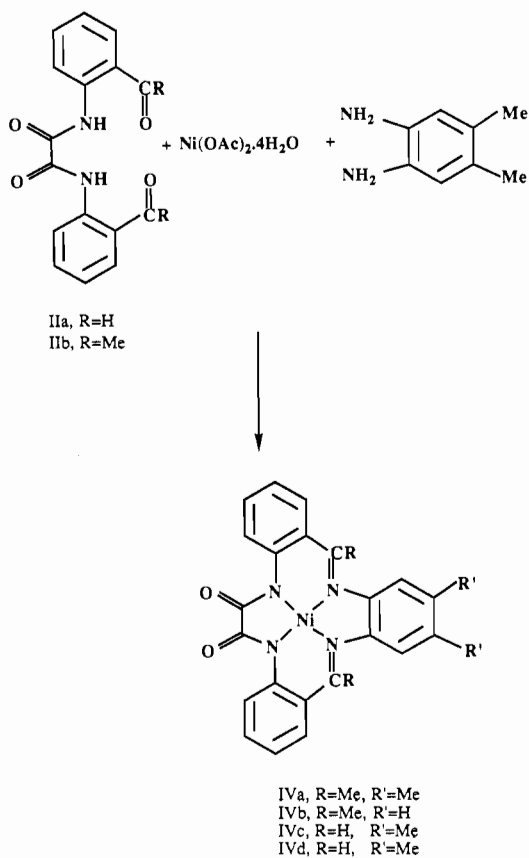
Co(α-diketo-TAD-Me$_2$) (Scheme I; IV, M = Co, R = H). The Co^{II} macrocyclic complex was prepared by the reaction of the macrocyclic ligand III and Co(OAc)$_2$·4H$_2$O in 1:1 molar ratio. III (0.384 g, 0.97 mM) and Co(OAc)$_2$.4H$_2$O (0.241 g, 0.97 mM) were dissolved in about 25 mL of distilled and degassed DMF under prepurified N$_2$. The reaction mixture was heated under N$_2$ at 95 °C in a vessel equipped with a reflux condenser for 16 h. The resulting red brick solution was cooled to 0 °C and following the addition of ~100 mL of distilled diethyl ether deposited a red-brown solid. Yield: 0.42 g; 97%. Single crystals were obtained by the slow diffusion of diethyl ether to a DMF solution of the compound, over a period of a few days.

Anal. Calcd for CoC$_{24}$H$_{18}$N$_4$O$_2$ (mol wt 453): C, 63.57; H, 3.97; N, 12.36; Co, 13.02. Found: C, 59.62; H, 3.93, N, 11.46; Co, 12.67.

The mass spectrum of the single crystals showed the presence of the parent ion peak, m/e = 453. This compound is X-ray isomorphous with the Ni^{II} analogue, which was obtained by a template reaction (Scheme II; IVc).

X-ray powder pattern spacings (Å): 11.5 (vs), 10.5 (vs), 5.4 (w), 5.1 (w), 4.7 (m), 4.1 (w), 3.4 (s), 3.25 (s), 2.6 (vw), 1.98 (vw).

FT-IR (cm^{-1}): 2972 (w), 2923 (w), 1656 (s), 1610 (vs), 1600 (vs), 1566 (vs), 1546 (vs), 1477 (w), 1444 (s), 1353 (vs), 1268 (w), 1208 (w), 1208 (w), 1183 (w), 1159 (m), 1113 (w), 1004 (w), 919 (w), 861 (m), 756 (vw), 679 (w), 603 (w), 578 (w), 530 (w), 516 (w), 468 (w).

Ni(α-diketo-TAD-Me$_4$) (Scheme II; IVa). This complex was prepared by the template reaction of the ligand precursor 2,2′-(oxalyldiimino)-bis(acetophenone) (Scheme I; IIb), Ni(OAc)$_2$·4H$_2$O, and 4,5-dimethyl-*o*-phenylenediamine, as described by Black et al.[18] The above template reaction (Scheme II) failed for metal ions other than Ni^{II}, such as Co^{II}, Fe^{II}, Cu^{II}, and Zn^{II}.

2,2′-(Oxalyldiimino)bis(acetophenone) (5.20 g, 16 mM), 4,5-dimethyl-*o*-phenylenediamine (3.12 g, 23 mM), and Ni(OAc)$_2$·4H$_2$O (2.84 g, 11 mM) were placed in 70 mL of DMF at 120 °C under N$_2$ for 24 h. The dark green reaction solution was cooled to 0 °C, and 10 mL of ice-cold MeOH was added. The green microcrystalline product that precipitated was filtered out and dried. Yield: 6.35 g; 82%.

Anal. Calcd for NiC$_{26}$H$_{22}$N$_4$O$_2$ (mol wt 480.7): C, 64.90; H, 4.57; N, 11.65; Ni, 12.21. Found: C, 64.68; H, 4.53; N, 10.52.

FT-IR (cm^{-1}): 3146 (w), 2864 (w), 1669 (vs), 1599 (m), 1576 (s), 1536 (s), 1512 (s), 1450 (s), 1140 (s), 1359 (vs), 1313 (m), 1255 (s), 1170 (m), 1083 (w), 1022 (w), 963 (w), 831 (w), 804 (w), 762 (s), 737 (s), 611 (m), 490 (m).

^{1}H NMR in DMSO-d_6 (ppm): 8.75 (d, arom), 8.66 (d, arom), 8.16 (d, arom), 8.00 (d, arom), 7.97 (s, arom), 7.27 (t, arom), 7.42 (t, arom),

7.35 (s, arom), 7.03 (t, arom), 2.88 (d, -Me), 2.25 (d, -Me).

Et$_4$N[Ni(α-diketo-TAD-Me$_4$+H)]·0.8CH$_3$COCH$_2$OHC(CH$_3$)$_2$ (Scheme III; V). This reaction was carried out under N$_2$ in a glovebox. Ni(α-diketo-TAD-Me$_4$) (1.15 g, 2.4 mM) and Et$_4$NBH$_4$ (0.7 g, 4.8 mM) were dissolved in about 50 mL of distilled acetone and stirred for 45 min. About 0.4 g of unreacted starting material was filtered off, and the resulting purple solution was layered with 200 mL of distilled diethyl ether. Large deep purple crystals formed overnight. Yield: 0.63 g; 39%.

Anal. Calcd for C$_{34}$H$_{43}$N$_5$O$_2$Ni·0.8C$_6$H$_{12}$O$_2$ (mol wt. 704.5): C, 65.94; H, 6.90; N, 9.86; Ni, 8.27. Found: C, 63.43; H, 6.97; N, 9.85; Ni, 8.03.

X-ray powder pattern spacings (Å): 14.0 (vs), 11.0 (s), 7.0 (s), 6.0 (w), 5.2 (vw), 4.1 (m), 3.9 (vw), 3.35 (vw).

FT-IR (cm^{-1}): 3400 (w), 3864 (w), 1699 (w), 1644 (vs), 1627 (vs), 1589 (s), 1493 (s), 1447 (m), 1360 (vs), 1313 (m), 1171 (w), 1047 (w), 1000 (w), 760 (s), 482 (w).

^{1}H NMR in DMSO-d_6 (ppm): 8.72 (d, arom), 7.79 (d, arom), 7.68 (d, arom) 7.22 (t, arom), 7.13 (t, arom), 6.90 (m, arom), 6.60 (s, arom), 4.57 (br s, -OH (aldol)), 4.36 (q, *H*C(CH$_3$)N), 2.9 (q, Et$_4$N$^+$), 2.55 (s, C*H*$_3$C=N), 2.07 (d, -Me), 1.30 (d, HC(C*H*$_3$)N), 1.14 (t, Et$_4$N$^+$).

[(5-crown-15)Na][Ni(α-diketo-TAD-Me$_4$+H)] (Scheme III; VI). This reaction was also carried out under N$_2$ in a glove box. Sodium amalgam was prepared by dissolving 0.12 g (5 mM) of sodium metal in about 40 mL of mercury. A 50-mL portion of distilled THF was added to the amalgam. A 0.82-g (1.7 mM) amount of Ni(α-diketo-TAD-Me$_4$) and 0.4 mL (2 mM) of 15-crown-5 were dissolved in the solvent, and the reaction was stirred for 2 h. The amalgam was filtered off, and the resulting purple solution was layered with ~200 mL of distilled diethyl ether. The ether was allowed to diffuse slowly over a period of 5 days, and large prismatic deep purple crystals were obtained. Yield: 0.29 g; 24%.

Anal. Calcd for NiC$_{36}$H$_{42}$N$_4$O$_7$Na (mol wt 724.7): C, 59.6; H, 5.93; N, 7.73; Ni, 8.1; Na, 3.17. Found: C, 59.47; H, 5.77; N, 7.43; Ni, 7.89; Na, 3.10.

X-ray powder pattern spacings (Å): 10.0 (vs), 8.5 (w), 6.8 (s), 4.8 (m), 4.5 (m), 3.95 (s), 3.6 (w), 3.45 (w), 3.2 (vw).

FT-IR (cm^{-1}): 2913 (m), 1636 (s), 1620 (vs), 1594 (s), 1492 (s), 1451 (m), 1416 (m), 1352 (vs), 1310 (vs), 1258 (s), 1118 (vs), 1101 (vs), 1047 (w), 945 (m), 877 (w), 862 (w), 816 (m), 757 (s), 485 (w).

^{1}H NMR in DMSO-d_6 (ppm): 8.72 (d, arom), 7.82 (d, arom), 7.70 (d, arom) 7.22 (t, arom) 7.07 (d, arom), 6.98 (m, arom) 6.79 (d, arom) 6.55 (s, arom) 4.36 (q, *H*C(CH$_3$)N), 3.54 (s, 5-crown), 2.81 (s, -Me), 2.06 (d, -Me), 1.34 (d, -Me).

Ni(α-diketo-TAD-Me$_4$)ZnCl$_2$·DMF (Scheme III; VII). Ni(α-diketo-TAD-Me$_4$) (0.45 g, 0.94 mM) was dissolved in 40 mL of acetone, and the solution was added to a solution of 0.16 g (1.2 mM) of ZnCl$_2$ in 40 mL of acetone. The reaction was stirred for about 10 min. The solution rapidly changed to red and a microcrystalline red solid precipitated out leaving a clear supernatant liquid. The product was filtered out and washed with acetone and ether. Yield: 0.55 g; 96%. This product is insoluble in all common solvents and dissolves in DMF with dissociation of ZnCl$_2$. Single crystals were obtained from a DMF solution in the presence of excess ZnCl$_2$ by slow diffusion of diethyl ether.

Anal. Calcd for (ZnCl$_2$)C$_{26}$H$_{22}$N$_4$O$_2$ (mol wt 617): C, 50.56; H, 3.56; N, 9.07. Found: C, 49.57; H, 3.67, N, 8.63.

X-ray powder pattern spacings (Å): 11.5 (vs), 9.2 (s), 8.8 (w), 7.70 (w), 7.30 (w), 6.4 (w), 5.8 (m), 4.5 (vw) 4.65 (w), 4.4 (w), 4.15 (s), 3.8 (s), 3.65 (w), 3.2 (w), 3.08 (vw), 2.85 (w), 2.75 (w), 2.2 (vw), 2.18 (vw).

FT-IR (cm^{-1}): 2925 (w), 1708 (m), 1667 (m), 1611 (vs), 1606 (vs), 1588 (m), 1537 (m), 1484 (w), 1442 (w), 1358 (s), 1332 (m), 1278 (m), 1225 (w), 1172 (w), 1096 (w), 1018 (w), 939 (w), 866 (w), 763 (s), 747 (s), 602 (w), 533 (w), 514 (m), 480 (m), 467 (m), 388 (m), 290 (m).

Ni(α-diketo-TAD-Me$_4$)Cu(NO$_3$)$_2$ (Scheme III; VIII). A 0.5-g (1 mM) amount of the green Ni macrocycle was stirred in 50 mL of acetone, and a solution of 0.25 g (1.3 mM) of CuNO$_3$·3H$_2$O in 10 mL of acetone was added. The reaction was swirled briefly, and all reagents went into solution with concomitant color change to deep red. The reaction solution was quickly filtered through filter paper to remove a residue of unreacted starting material. Crystallization began immediately; the filtrate was refrigerated overnight, and the red microcrystalline product was collected on a coarse fritted funnel, washed with two portions of acetone and one portion of ether, and dried in the air. Yield: 0.26 g; 37%.

Anal. Calcd for NiC$_{26}$H$_{22}$N$_7$O$_8$Cu (mol wt 668.2): C, 46.69; H, 3.29; N, 12.57; Ni, 8.78; Cu, 9.50. Found: C, 45.52; H, 3.58; N, 12.10; Ni, 8.38; Cu, 9.19.

X-ray powder pattern spacings (Å): 13.0 (s), 9.0 (vs), 8.0 (m), 4.8 (w), 4.1 (w), 3.9 (w), 3.5 (w), 3.3 (w), 2.1 (vw).

FT-IR (cm^{-1}): 3281 (br, w), 2864 (w), 1616 (vs), 1585 (s), 1578 (s), 1533 (s), 1497 (vs), 1487 (vs), 1448 (s), 1432 (s), 1404 (vs), 1361 (n, s), 1321 (vs), 1290 (s), 1276 (s), 1236 (w), 1018 (s), 1007 (s), 880 (m),

Scheme III

V

VI

Ni^{II}(α-diketo-TAD-Me$_4$)

IVa

VII

VIII
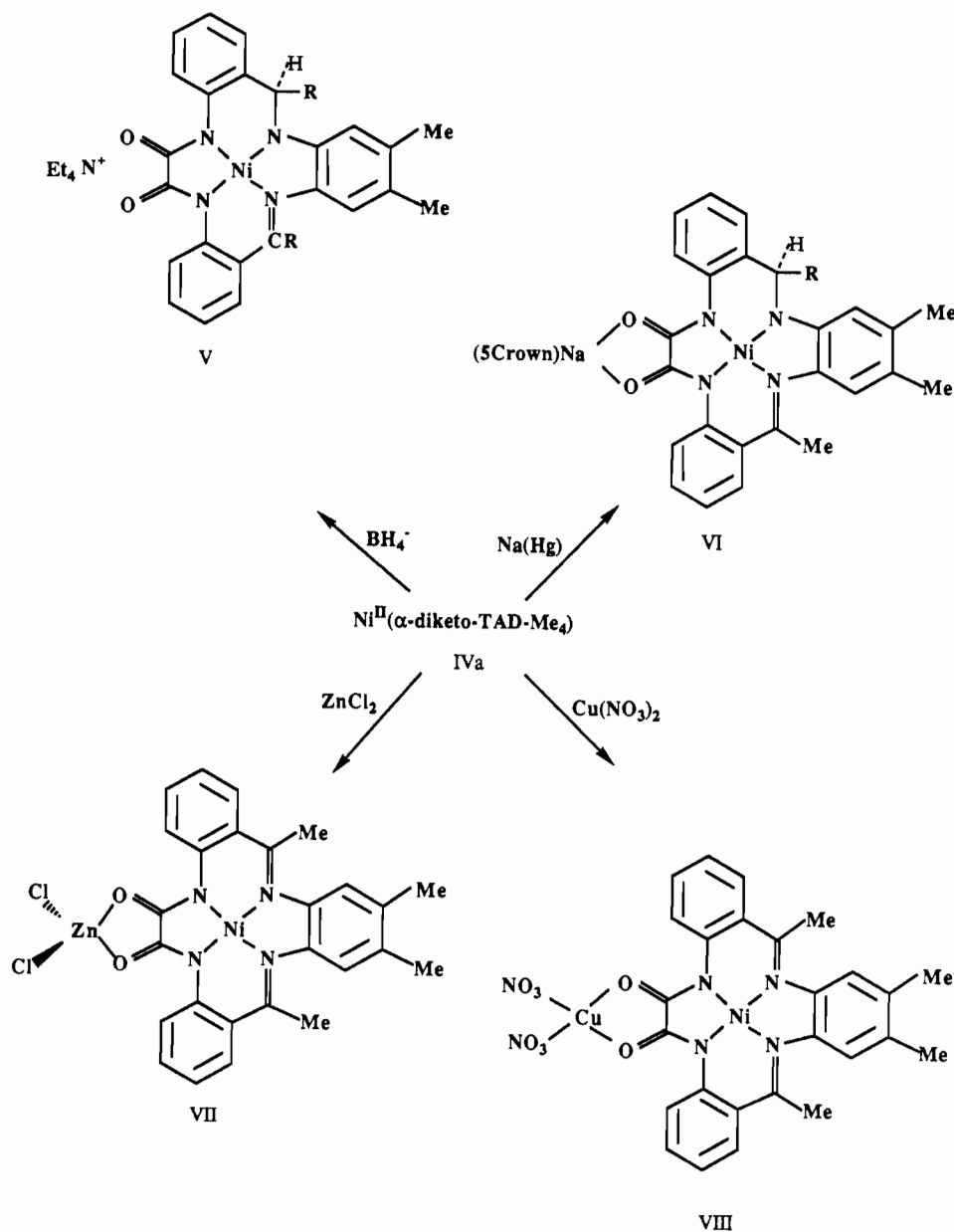
803 (m), 770 (n, s), 589 (m), 480 (m).

X-ray Diffraction Measurements. Collection of Data. Single crystals of IVa (Scheme II) were obtained by the slow diffusion of diethyl ether into an acetone solution of the complex. Crystals of VII (Scheme III) were obtained by the slow diffusion of diethyl ether into a DMF solution of the compound containing an excess of ZnCl$_2$. For V and VI (Scheme III) single crystals came out of the reaction mixtures as described in their syntheses. The crystals used for data collection were sealed in quartz capillaries. Details concerning the crystal characteristics, the data collection, and the structure refinement are shown in Table I. Intensity data for IVa–VII were obtained on a Nicolet P3/F four-circle diffractometer. The instrument and the data acquisition procedures have been described earlier.[20]

Reduction of Data. The raw data were reduced to net intensities, estimated standard deviations were calculated on the basis of counting statistics, Lorentz and polarization corrections were applied, and equivalent reflections were averaged. The estimated standard deviation of the structure factor was taken as the larger of that derived from counting statistics and of that derived from the scatter of multiple measurements. The weighting function used throughout the refinement of the structure gives zero weight to those reflections with $F^2 < 3\sigma(F)^2$ and $w = 1/\sigma^2(F)$ to all others $\sigma^2(F^2) = (0.06F^2)^2 + \sigma^2(F^2)$ (from counting statistics).[21]

The scattering factors of the neutral non-hydrogen atoms were taken from the tables of Doyle and Turner,[22] and real and imaginary dispersion corrections[23] were applied to all of them. The spherical hydrogen scattering factor tables of Stewart, Davidson, and Simpson[24] were used. In view of the small values of μ, no absorption correction was applied to any of the data sets.

Determination of the Structures. Ni(α-diketo-TAD-Me$_4$). The structure of Ni(α-diketo-TAD-Me$_4$) was determined by using data collected to $2\theta_{max} = 45°$. The molecule has mirror symmetry, and the metal atom resides on a crystallographic mirror plane. The heavy atom was located in the Patterson map. The Ni coordinates were input into a structure factor calculation, and following two Fourier syntheses the rest of the non-hydrogen atoms in the asymmetric unit were located. Refinement of all atoms in the asymmetric unit by full-matrix least-squares techniques using isotropic temperature factors converged to an R value of 0.09. Anisotropic refinement of all atoms gave an R value of 0.056. A difference Fourier map revealed the positions of all hydrogen atoms. The hydrogen atoms were included in the structure factor calculation with fixed temperature factors but were not refined. Final refinement resulted in an R value of 0.044. The weighted R value was 0.043. During the last cycle of refinement all parameter shifts were less than 10% of their esd's.

(20) Kanatzidis, M. G.; Coucouvanis, D. *Inorg. Chem.* **1984**, *23*, 403.
(21) Grant, D. F.; Killean, R. C. G.; Lawrence, J. L. *Acta Crystallogr., Sect. B* **1969**, *B25*, 374.
(22) Doyle, P. A.; Turner, P. S. *Acta Crystallogr., Sect. A* **1968**, *A24*, 390.
(23) Cromer, D. T.; Liberman, D. J. *J. Chem. Phys.* **1970**, *53*, 1891.
(24) Stewart, R. F.; Davidson, E. R.; Simpson, W. T. *J. Chem. Phys.* **1965**, *42*, 3175.

Table I. Summary of Crystal Data, Intensity Collection, and Structure Refinement Data for Ni(α-diketo-TAD-Me$_4$) (IVa),[a] Et$_4$N[Ni(α-diketo-TAD-Me$_4$+H)]·0.8C$_6$H$_{12}$O$_2$ (V), [Na(5-crown-15)][Ni(α-diketo-TAD-Me$_4$+H)] (VI), and [Ni(α-diketo-TAD-Me$_4$)]ZnCl$_2$·HCON(Me)$_2$ (VII)

	IVa	V	VI	VII
chem formula	NiO$_2$N$_4$C$_{26}$H$_{22}$	NiO$_2$N$_5$C$_{34}$H$_{43}$·0.8C$_6$H$_{12}$O$_2$	NiNaO$_7$N$_4$C$_{36}$H$_{43}$	NiZnCl$_2$O$_2$N$_4$C$_{26}$H$_{22}$·C$_3$H$_7$NO
mol wt	480.7	704.5	724.7	689.7
space group	*Pnam*	*P2$_1$/a*	*P2$_1$/n*	*P2$_1$/c*
a, Å	7.934 (4)	14.789 (6)	17.201 (11)	11.139 (9)
b, Å	12.663 (6)	17.582 (5)	12.113 (11)	16.192 (19)
c, Å	20.922 (9)	15.372 (6)	17.426 (12)	16.149 (14)
α, deg	90.00	90.00	90.0	90.00
β, deg	90.00	108.36 (3)	75.32 (5)	98.03 (7)
γ, deg	90.00	90.00	90.00	90.00
Z; *V*, Å^3	4; 2102	4; 3793	4; 3512	4; 2884
d_{obsd}, g/cm^3 [b]	1.50 (2)	1.25 (2)	1.33 (2)	1.40 (2)
d_{calcd}, g/cm^3	1.52	1.23	1.37	1.31
radiation	Mo Kα[c]	Mo Kα[c]	Mo Kα[c]	Mo Kα[c]
cryst dimens, mm		0.82 × 0.21 × 0.24	0.55 × 0.30 × 0.25	0.21 × 0.15 × 0.18
μ, cm^{-1}	9.25	5.23	5.92	16.8
data collcd	+*h*,+*k*,±*l*	+*h*,+*k*,±*l*	+*h*,+*k*,±*l*	+*h*,±*k*,±*l*
$2\theta_{max}$, deg	45	40	45	40
no. of unique rflcns	1436	3511	4621	2711
no. of reflcns with $I > 3\sigma(I)$	1085	2455	2440	1514
no. of atoms in asymm unit	17	50	49	41
no. of variables	151	371	349	215
R, *R*$_w$[d]	0.044, 0.043	0.073, 0.072	0.078, 0.075	0.073, 0.067

[a] The code for the abbreviated names of the complexes is given in the introduction, and the numbers refer to entires in Schemes II and III. [b] Density determined by flotation in a CCl$_4$/pentane mixture. [c] $\lambda = 0.709\,26$ Å. [d] $R = \sum(F_o - |F_c|)/\sum F_o$; $R_w = \sum((F_o - |F_c|)^2/\sum F_o^2)^{1/2}$.

Et$_4$N[Ni(α-diketo-TAD-Me$_4$+H)]·0.8C$_6$H$_{12}$O$_2$ (Scheme III; V). The structure of V was solved from the Patterson map. The anion is sitting on a general position. The Ni coordinates were input, and subsequent Fourier syntheses located all the non-hydrogen atoms for the anion and the tetraethylammonium cation. Isotropic refinement of all atoms gave an *R* value of 0.16. A third molecule appeared in the difference Fourier map and was input as a diacetone alcohol molecule (after its presence in the crystals was verified by a mass spectrum where it appeared as the only volatile constituent) and refined. Anisotropic refinement of all atoms in the anion and of the cation nitrogen atom and isotropic refinement of the remaining non-hydrogen atoms resulted in an *R* value of 0.094. Input of the hydrogen atoms in the structure factor calculation at their calculated positions gave an *R* value of 0.082. The diacetone alcohol molecule was best refined with occupancy 0.8, and it had high thermal parameters. The *R* value converged to 0.073, and during the last cycle of refinement all parameter shifts were less than 10% of their esd's.

[(5-crown-15)Na][Ni(α-diketo-TAD-Me$_4$+H)] (Scheme III; VI). The structure of VI was solved from the Patterson synthesis map from data collected to $2\theta_{max} = 40°$. The Ni coordinates were input, and two subsequent Fourier syntheses located all the non-hydrogen atoms for the anion, the Na atom, and part of the crown ether molecule, which appeared to be disordered. All atoms in the anion, the sodium atom, and five oxygens from the crown ether molecule were input, and after one cycle of least-squares refinement the *R* value was lowered from 0.394 to 0.229. After the input of six carbon atoms of the crown molecule and two additional cycles the *R* value was 0.133. At this point it became clear that the crown ether molecule was indeed disordered. Additional (–C–C–) components were found and input with partial occupancy. Anisotropic refinement on 18 atoms including Ni, Na, and 4 N gave an *R* value of 0.095. To solve the problem of the cation disorder, a second data set was collected on a different crystal to $2\theta_{max} = 45°$. Input of the atomic coordinates and least-squares refinement using the new data set gave an *R* value of 0.109. The best model for the disordered crown molecule consisted of three components with occupancies 0.5, 0.3, and 0.2. For the minor components the temperature factors and also the carbon–carbon and oxygen–carbon distances were fixed. After calculation of the hydrogen atoms and additional least-squares refinements, the *R* value converged to 0.078, and during the last cycle of refinement all parameter shifts were less than 10% of their esd's.

[Ni(α-diketo-TAD-Me$_4$)]ZnCl$_2$·DMF (Scheme III; VII). The structure of [Ni(α-diketo-TAD-Me$_4$)]ZnCl$_2$·DMF was determined by using data collected to $2\theta_{max} = 40°$. The molecule is situated on a general position. The solution of the structure was suggested by the direct methods routine SOLV of the SHELXTL[25] crystallographic package, and the positions of the heavy atoms were verified in the Patterson map. Initially 26 atoms were input, including Zn, Ni, 4 N and 2 O. The Fourier synthesis map

(25) SHELXTL package of crystallographic programs, Nicolet XRD Corp., Fremont, CA.

Table II. Fractional Atomic Coordinates for Ni(α-diketo-TAD-Me$_4$)

atom	x	y	z	U_{eq},[a] Å^2
Ni	0.0366 (1)	0.2155 (0)	0.2500 (0)	0.034
N(1)	0.0286 (4)	0.3210 (2)	0.3108 (1)	0.040
N(2)	0.0473 (4)	0.01077 (2)	0.3110 (1)	0.036
C(1)	0.0932 (4)	0.4126 (3)	0.2870 (2)	0.047
C(2)	−0.0241 (5)	0.3095 (3)	0.3738 (2)	0.043
C(3)	−0.0498 (6)	0.3987 (3)	0.4128 (2)	0.060
C(4)	−0.1194 (7)	0.3883 (5)	0.4726 (3)	0.077
C(5)	−0.1624 (6)	0.2922 (5)	0.4971 (2)	0.079
C(6)	−0.1342 (6)	0.2045 (4)	0.4610 (2)	0.064
C(7)	−0.0633 (4)	0.2085 (3)	0.3989 (2)	0.044
C(8)	−0.0208 (4)	0.1089 (3)	0.3681 (2)	0.041
C(9)	−0.0579 (6)	0.0076 (4)	0.4025 (2)	0.056
C(10)	0.1253 (4)	0.0170 (3)	0.2835 (2)	0.037
C(11)	0.2159 (5)	−0.0601 (3)	0.3156 (2)	0.047
C(12)	0.3053 (4)	−0.1365 (3)	0.2835 (2)	0.054
C(13)	0.4067 (8)	−0.2167 (5)	0.3201 (3)	0.085
O(1)	0.1440 (4)	0.4904 (2)	0.3152 (1)	0.066

[a] Equivalent isotropic termpature factor U_{eq} defined as one-third of the trace of the orthogonal U_{ij} tensor for all.

revealed the two chlorine atoms bound tetrahedrally to Zn. Subsequent Fourier syntheses revealed the rest of the carbon atoms and a DMF solvent molecule. Isotropic refinement of all non-hydrogen atoms converged to $R = 0.097$. Anisotropic refinement of all non-hydrogen atoms, with the H atoms included in the structure factor calculation but not refined, converged to a final *R* value of 0.074. During the last cycle of refinement all parameter shifts were less than 10% of their esd's.

Crystallographic Results. The final atomic positional and thermal parameters of the non-hydrogen atoms in Ni(α-diketo-TAD-Me$_4$) (IVa), Et$_4$N[Ni(α-diketo-TAD-Me$_4$+H)]·0.8C$_6$H$_{12}$O$_2$ (V), [(5-crown-15)-Na][Ni(α-diketo-TAD-Me$_4$+H)] (VI), and [Ni(α-diketo-TAD-Me$_4$)]-ZnCl$_2$·DMF (VII), with standard deviations derived from the inverse matrices of the least-squares refinements, are compiled in Tables II–V, respectively. Intramolecular distances and angles for all of the above are compiled in Table VI. The structure-labeling schemes and packing diagrams are shown in Figures 1–6.

Results and Discussion.

Synthesis and Characterization. The syntheses of the ligands and the macrocyclic complexes are outlined in the reaction Schemes I–III. The free macrocyclic ligand (Scheme I; III) was prepared by high-dilution techniques in DMF. The choice of the solvent was dictated by the fact that the ligand precursor 2,2′-(oxalyldiimino)bis(benzaldehyde) (Scheme I; IIa) is soluble only in hot DMF. When this reaction was carried out in solvents such

Table III. Fractional Atomic Coordinates for
$Et_4N^+[Ni(\alpha\text{-diketo-TAD-Me}_4+H)]^-\cdot 0.8CH_3COCH_2OHC(CH_3)_2$

atom	x	y	z	U_{eq},[a] Å^2
Ni	0.3563 (01)	0.6008 (01)	0.1506 (01)	0.043
N(1)	0.3708 (06)	0.5007 (05)	0.1911 (05)	0.047
N(2)	0.4562 (05)	0.6336 (05)	0.2471 (05)	0.045
Nn(3)	0.3638 (05)	0.6955 (04)	0.0975 (06)	0.037
N(4)	0.2434 (05)	0.5684 (05)	0.0648 (05)	0.040
N(5)	0.2133 (05)	0.9198 (05)	0.1743 (05)	0.059
O(1)	0.2806 (05)	0.3892 (04)	0.1698 (05)	0.062
O(2)	0.1505 (05)	0.4587 (04)	0.0259 (05)	0.059
C(1)	0.2954 (08)	0.4563 (06)	0.1508 (07)	0.049
C(2)	0.4544 (07)	0.4667 (06)	0.2506 (07)	0.045
C(3)	0.4840 (08)	0.3949 (06)	0.2384 (07)	0.058
C(4)	0.5680 (09)	0.3656 (06)	0.2955 (10)	0.074
C(5)	0.6256 (08)	0.4094 (07)	0.3672 (08)	0.068
C(6)	0.5983 (08)	0.4822 (07)	0.3793 (07)	0.059
C(7)	0.5128 (08)	0.5129 (06)	0.3207 (07)	0.051
C(8)	0.4902 (07)	0.5945 (06)	0.3344 (06)	0.055
C(9)	0.4174 (08)	0.6007 (06)	0.3864 (07)	0.079
C(10)	0.4816 (06)	0.7061 (06)	0.2394 (07)	0.044
C(11)	0.5501 (07)	0.7506 (06)	0.3072 (06)	0.052
C(12)	0.5723 (07)	0.8236 (06)	0.2915 (07)	0.051
C(13)	0.6434 (07)	0.8674 (07)	0.3677 (08)	0.075
C(14)	0.5275 (07)	0.8584 (06)	0.2055 (08)	0.055
C(15)	0.5509 (07)	0.>396 (06)	0.1875 (07)	0.062
C(16)	0.4607 (07)	0.8161 (06)	0.1408 (06)	0.044
C(17)	0.4365 (06)	0.7426 (06)	0.1547 (06)	0.038
C(18)	0.3241 (07)	0.7077 (05)	0.0094 (07)	0.041
C(19)	0.3690 (07)	0.7550 (06)	-0.0469 (06)	0.060
C(20)	0.2278 (07)	0.6768 (06)	-0.0388 (07)	0.049
C(21)	0.1724 (08)	0.7149 (05)	-0.1178 (07)	0.053
C(22)	0.0788 (09)	0.6960 (07)	-0.1596 (07)	0.059
C(23)	0.0359 (07)	0.6407 (07)	-0.1228 (09)	0.061
C(24)	0.0883 (08)	0.5999 (06)	-0.0480 (07)	0.056
C(25)	0.1866 (07)	0.6147 (06)	-0.0060 (07)	0.046
C(26)	0.2186 (07)	0.4956 (06)	0.0738 (07)	0.045
C(27)	0.1947 (08)	0.4616 (07)	-0.1894 (08)	0.075
C(28)	0.1712 (09)	0.5211 (08)	-0.2632 (09)	0.100
C(29)	0.2855 (08)	0.3749 (06)	-0.2577 (08)	0.070
C(30)	0.2111 (09)	0.3120 (07)	-0.2818 (08)	0.095
C(31)	0.2971 (08)	0.3715 (06)	-0.0911 (08)	0.071
C(32)	0.3860 (09)	0.3213 (07)	-0.0630 (08)	0.091
C(33)	0.3700 (07)	0.4736 (06)	-0.1580 (07)	0.064
C(34)	0.3842 (08)	0.5296 (07)	-0.0791 (08)	0.090
C(35)	0.0428 (30)	0.3750 (20)	0.4262 (26)	0.281
C(36)	0.1433 (29)	0.3664 (20)	0.4574 (24)	0.240
O(3)	0.1743 (12)	0.4190 (10)	0.5199 (13)	0.193
C(37)	0.2251 (17)	0.3152 (14)	0.4559 (17)	0.169
C(38)	0.2594 (15)	0.3288 (13)	0.3819 (14)	0.124
C(39)	0.1903 (10)	0.3320 (08)	0.2967 (10)	0.073
C(40)	0.3258 (16)	0.2741 (14)	0.3762 (15)	0.164
O(4)	0.3013 (16)	0.4051 (13)	0.3914 (16)	0.273

[a] Equivalent isotropic temperature factor U_{eq} defined as one-third of the trace of the orthogonal U_{ij} tensor for all.

Table IV. Fractional Atomic Coordinates for
$[(5\text{-crown-15})Na][Ni(\alpha\text{-diketo-TAD-Me}_4+H)]$

atom	x	y	z	U_{eq},[a] Å^2
Ni	0.3829 (01)	0.9563 (01)	0.0319 (01)	0.047
Na	0.1441 (03)	1.2150 (05)	0.1146 (04)	0.082
N(1)	0.2777 (06)	1.0012 (08)	-0.0200 (06)	0.047
N(2)	0.3803 (07)	0.8367 (09)	-0.0346 (07)	0.060
N(3)	0.4890 (06)	0.9091 (09)	0.0823 (06)	0.052
N(4)	0.3760 (06)	1.0658 (08)	0.1060 (05)	0.050
O(1)	0.1739 (06)	1.1033 (08)	0.0064 (06)	0.075
O(2)	0.2744 (06)	1.1489 (08)	0.1514 (05)	0.078
C(1)	0.2429 (10)	1.0651 (12)	0.0238 (08)	0.055
C(2)	0.2415 (08)	0.9825 (12)	-0.1027 (08)	0.048
C(3)	0.1975 (08)	1.0626 (12)	-0.1496 (08)	0.057
C(4)	0.1658 (08)	1.0443 (15)	-0.2305 (09)	0.066
C(5)	0.1774 (09)	0.9466 (17)	-0.2636 (08)	0.076
C(6)	0.2250 (09)	0.8655 (14)	-0.2169 (09)	0.074
C(7)	0.2579 (08)	0.8817 (13)	-0.1354 (08)	0.051
C(8)	0.3076 (09)	0.7897 (12)	-0.0889 (08)	0.059
C(9)	0.2589 (09)	0.7214 (12)	-0.0447 (10)	0.076
C(10)	0.4477 (09)	0.7767 (12)	-0.0189 (07)	0.050
C(11)	0.4641 (09)	0.6793 (13)	-0.0554 (08)	0.060
C(12)	0.5401 (11)	0.6362 (12)	-0.0426 (09)	0.068
C(13)	0.5536 (09)	0.5342 (14)	-0.0883 (09)	0.090
C(14)	0.6060 (09)	0.6878 (14)	0.0111 (10)	0.063
C(15)	0.6915 (09)	0.6463 (14)	0.0217 (09)	0.088
C(16)	0.5894 (08)	0.7765 (13)	0.0517 (08)	0.053
C(17)	0.5129 (09)	0.8189 (11)	0.0430 (08)	0.049
C(18)	0.5287 (07)	0.9419 (11)	0.1546 (08)	0.051
C(19)	0.5923 (09)	0.8690 (12)	0.2064 (09)	0.074
C(20)	0.5126 (08)	1.0456 (12)	0.1868 (07)	0.054
C(21)	0.5789 (09)	1.0903 (14)	0.2448 (09)	0.083
C(22)	0.5702 (11)	1.1887 (15)	0.2785 (10)	0.099
C(23)	0.5018 (10)	1.2487 (14)	0.2592 (09)	0.090
C(24)	0.4344 (09)	1.2076 (12)	0.2017 (08)	0.071
C(25)	0.4419 (08)	1.1049 (11)	0.1670 (08)	0.056
C(26)	0.3002 (09)	1.0799 (12)	0.1023 (09)	0.054
O(3)	0.0189 (32)	1.2951 (42)	-0.0076 (29)	0.138
O(4)	0.0118 08)	1.1199 (12)	0.0790 (09)	0.146
O(5)	0.3954 (11)	0.6457 (15)	0.2657 (11)	0.118
O(6)	0.1776 (11)	1.3449 (15)	0.2377 (11)	0.188
O(7)	0.1638 (17)	1.4255 (22)	0.0784 (17)	0.144
C(27)	0.5145 (57)	0.7032 (61)	0.5225 (55)	0.187
C(28)	0.5437 (13)	0.6655 (18)	0.4783 (14)	0.132
C(29)	0.4956 (21)	0.5483 (34)	0.3599 (23)	0.102
C(30)	0.4876 (27)	0.6059 (40)	0.2917 (29)	0.111
C(31)	0.3808 (14)	0.7181 (20)	0.2053 (14)	0.138
C(32)	0.2925 (26)	0.7665 (44)	0.2073 (33)	0.140
C(33)	0.2588 (19)	0.9074 (25)	0.2705 (17)	0.150
C(34)	0.2961 (17)	0.9811 (25)	0.3322 (19)	0.150
C(35)	0.3861 (26)	0.9556 (35)	0.4919 (23)	0.139
C(36)	0.4349 (30)	0.8675 (41)	0.5349 (25)	0.115
O(8)	0.4610 (18)	0.8251 (25)	0.4784 (17)	0.092
O(9)	0.4519 (33)	0.6647 (43)	0.2600 (31)	0.160
O(10)	0.3140 (25)	0.9021 (31)	0.3900 (25)	0.068
C(37)	0.5174 (63)	0.7335 (82)	0.5416 (66)	0.160
C(38)	0.5308 (33)	0.6265 (47)	0.3565 (35)	0.085
C(39)	0.4526 (44)	0.5487 (49)	0.2986 (42)	0.117
C(40)	0.3188 (27)	0.7964 (36)	0.1911 (29)	0.104
C(41)	0.3668 (49)	0.9967 (57)	0.4412 (53)	0.160
C(42)	0.4013 (66)	0.9077 (78)	0.5045 (56)	0.160
C(43)	0.2760	0.9324	0.2937	0.160
C(44)	0.3041	0.9821	0.3763	0.160
C(45)	0.4658	0.5794	0.3274	0.160
C(46)	0.5568	0.5807	0.3813	0.160

[a] Equivalent isotropic temperature factor U_{eq} defined as one-third of the trace of the orthogonal U_{ij} tensor for all.

as EtOH or MeOH, insoluble materials along with small amounts of product were obtained. Employment of Zn^{2+} or other template ions, which had been used effectively in the cyclic Shiff-base condensations of similar ligand precursors[26] for the preparation of free macrocyclic ligands, was not useful in the synthesis of the free ligand (III).

A series of macrocyclic complexes (Scheme II; IV) were prepared from dialdehydes or diketones by the template reactions, as described previously.[18] The complexes IVa and IVb are green microcrystalline solids, and they are soluble in organic solvents. Unfortunately, complexes IVc and IVd, which are violet microcrystalline solids, are only sparingly soluble in DMF, CH_3CN, or dimethyl sulfoxide, DMSO, and solution studies could not be carried out. Complex IVa was soluble in DMF, CH_2Cl_2, and acetone and was used as a test molecule for a study of its interactions with Lewis acids. The Co^{II} macrocyclic complex was prepared by the reaction of the free ligand with $Co(OAc)_2\cdot 4H_2O$, and it was X-ray isomorphous with the analogous Ni^{II} complex

(26) Green, M.; Smith, J.; Tasker, P. A. *Inorg. Chim. Acta* **1971**, *5*, 17–24.

(Scheme II; IVc) that was prepared by the template reaction.

The α-diketo functionality in the ligand (III) potentially is available for ternary interactions of the Ni^{II} and Co^{II} macrocycles with Lewis acids. These interactions were investigated in weakly polar, noncoordinating solvents, such as acetone or CH_2Cl_2, with such Lewis acids as $ZnCl_2$, $Cu(NO_3)_2\cdot 3H_2O$, $FeCl_3$, $ZrCl_4$, and $SnCl_4$. In some instances ($FeCl_3$, $ZrCl_4$, $SnCl_4$) insoluble adducts were isolated that could not be purified by recrystallization. When these adducts dissolved in polar solvents, their dissolution was due
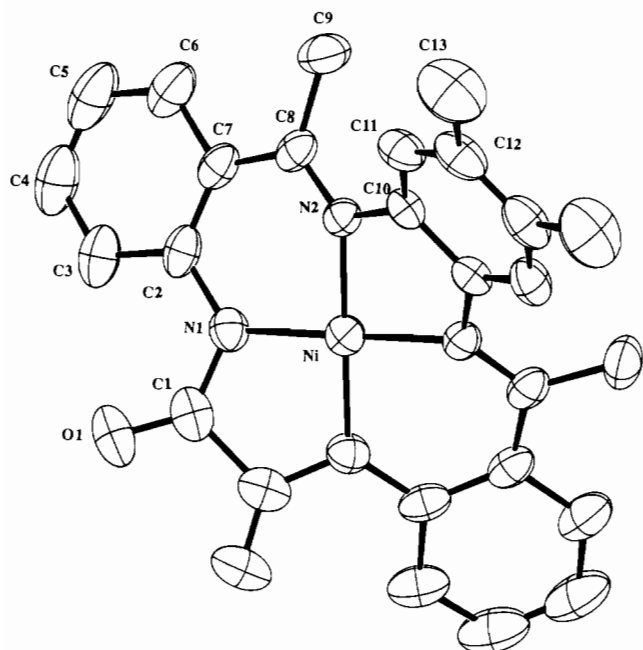
Figure 1. Structure of Ni(α-diketo-TAD-Me$_4$) as drawn by ORTEP[46] with thermal ellipsoids at the 50% probability level.

to solvolysis that resulted in their dissociation to parent macrocycles and the free Lewis acids.

The frequency of the ν(C=O) vibration is a feature in the infrared spectra of the complexes that can be used to monitor adduct formation. A bathochromic shift of about 60 cm^{-1} is observed in the ν(C=O) stretching frequencies of the ZnCl$_2$ and Cu(NO$_3$)$_2$ adducts consistent with localization of positive charge on the oxygen atoms. The far-IR spectrum of the ZnCl$_2$ adduct shows strong bands at 467, 388, and 290 cm^{-1}, which were assigned to ν(Ni-N), ν(Zn-O), and ν(Zn-Cl), respectively. The far-IR spectrum of the Cu(NO$_3$)$_2$ adduct was more complex with bands at 480, 454, 437, 408, 339, and 204 cm^{-1}.

The reduction of the macrocyclic complex was undertaken by using either borohydride or sodium amalgam. In both cases the formation of V and VI, respectively, was the result of hydrogenation of the imine function of the macrocyclic ring. This result has been attributed previously to the predominantly ligand character of the added electron that facilitates hydrogenation of the macrocyclic ring. Apparently, the presence of even one imine function is sufficient to lower the energy of the ligand π^* orbital relative to that of the metal d$_{x^2-y^2}$ σ^* orbital in these complexes.[27] Borohydride reductions are expected to at least partially saturate macrocyclic rings.[28] Similarly, electrochemical reduction in protic solvents leads to the hydrogenation of the imine functions of the macrocyclic rings.[29] The results of the sodium amalgam reduction were somewhat surprising in view of the fact that this reaction was carried out in a nonprotic medium (THF). The reduction of Ni(salophen) by sodium in THF has been reported[12c] to yield a carbon–carbon-bonded dimer. We can surmise that the absence of a radical reaction, in the sodium amalgam reduction of IVa, very likely is due to insufficient drying of the reaction solvent. During the synthesis of V, the acetone solvent underwent aldolic condensation due to either BH$_4^-$ attack or possibly attack by the IVa$^-$ species. A diacetone alcohol molecule was found incorporated in the crystal lattice of V.

Crystallographic Studies. The crystal structures of IVa, VI, and VII consist of discrete molecular units. In the structure of VII a DMF molecule of solvation is not involved in coordination. In the structure of V the anions, cations, and an unexpected
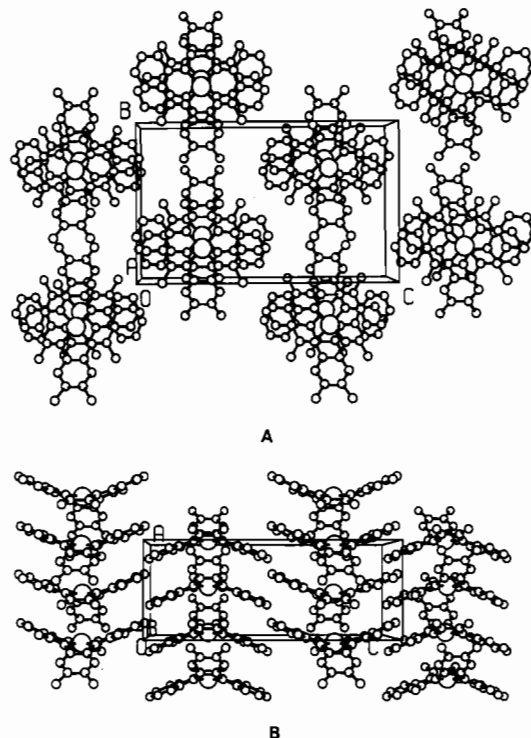

Figure 2. PLUTO[47] packing diagram of Ni(α-diketo-TAD-Me$_4$) in two orientations. The molecules are stacking along the a axis.
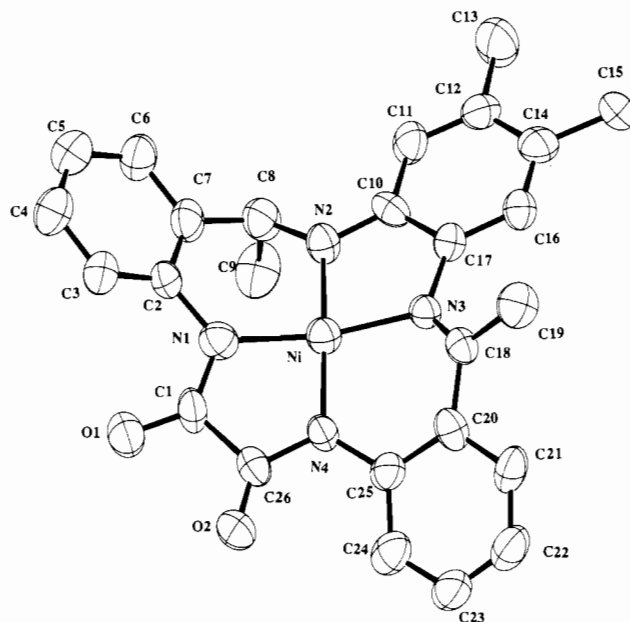

Figure 3. Structure of the [Ni(α-diketo-TAD-Me$_4$+H)]$^-$ anion as drawn by ORTEP with thermal ellipsoids at the 50% probability level.

molecule of diacetone alcohol are well separated in the lattice. The cations (in V) and the molecules of solvation (in V and VII) have expected unexceptional geometries and will not be considered further. Selected atomic distances and angles for the macrocyclic complexes are compiled in Table VI.

The crystal structure of IVa shows the macrocyclic molecules in a saddle-shaped conformation, stacked along the crystallographic a axis (Figures 1 and 2). A saddle conformation also is found in the structures of V–VII (Figures 3–6). Related [14]N_4 macrocycles (Figure 7a–c) are nearly planar[30,31] when unsub-

(27) Lovecchio, F. V.; Gore, E. S.; Busch, D. H. *J. Am. Chem. Soc.* **1974**, *96*, 3109–3118.
(28) Curtis, N. F. *J. Chem. Soc.* **1964**, 2644.
(29) Barefield, E. K.; Lovecchio, F. V.; Tokel, N. E.; Ochiai, E.; Busch, D. H. *Inorg. Chem.* **1972**, *11*, 283.

(30) Maslen, E. N.; Engelhardt, L. M.; White, A. H. *J. Chem. Soc., Dalton Trans.* **1974**, 1799–1803.
(31) (a) Goedken, V. L.; Pluth, J. J.; Peng, S. M.; Bursten, B. *J. Am. Chem. Soc.* **1976**, *98*, 8014–8021. (b) Weiss, M. C.; Bursten, B.; Peng, S. M.; Goedken, V. L. *Ibid.* **1976**, *98*, 8021–8031.

Table V. Fractional Atomic Coordinates for [Ni(α-diketo-TAD-Me$_4$)]ZnCl$_2$·DMF

atom	x	y	z	U_{eq},^{a} Å^2
Zn	0.1741 (2)	0.2233 (1)	0.3628 (2)	0.060
Ni	0.3935 (2)	0.5008 (2)	0.4245 (1)	0.041
Cl(1)	0.1901 (5)	0.0966 (3)	0.4054 (3)	0.076
Cl(2)	0.0419 (6)	0.2576 (4)	0.2556 (4)	0.096
O(1)	0.3365 (11)	0.2737 (7)	0.3466 (8)	0.066
O(2)	0.1792 (11)	0.3141 (7)	0.4493 (7)	0.054
N(1)	0.4351 (13)	0.4001 (9)	0.3802 (8)	0.043
N(2)	0.4895 (13)	0.5632 (9)	0.3594 (8)	0.042
N(3)	0.3337 (13)	0.6035 (8)	0.4550 (8)	0.043
N(4)	0.2842 (13)	0.4399 (8)	0.4760 (8)	0.040
C(1)	0.3536 (17)	0.3429 (12)	0.3849 (11)	0.037
C(2)	0.5319 (15)	0.3847 (10)	0.3323 (10)	0.033
C(3)	0.5949 (16)	0.3079 (10)	0.3333 (11)	0.046
C(4)	0.6799 (18)	0.2948 (11)	0.2854 (11)	0.058
C(5)	0.7175 (16)	0.3568 (11)	0.2394 (11)	0.048
C(6)	0.6645 (16)	0.4327 (11)	0.2385 (11)	0.047
C(7)	0.5746 (15)	0.4501 (11)	0.2875 (10)	0.036
C(8)	0.5335 (16)	0.5343 (11)	0.2938 (12)	0.047
C(9)	0.5481 (15)	0.5896 (11)	0.2186 (10)	0.045
C(10)	0.4869 (16)	0.6476 (11)	0.3788 (10)	0.037
C(11)	0.5723 (16)	0.7045 (10)	0.3592 (10)	0.041
C(12)	0.5731 (15)	0.7839 (11)	0.3891 (10)	0.040
C(13)	0.6679 (17)	0.8431 (11)	0.3693 (11)	0.056
C(14)	0.4899 (16)	0.8088 (10)	0.4395 (11)	0.042
C(15)	0.4833 (15)	0.8921 (11)	0.4743 (10)	0.047
C(16)	0.4035 (16)	0.7513 (10)	0.4596 (10)	0.045
C(17)	0.4007 (16)	0.6706 (10)	0.4276 (10)	0.033
C(18)	0.2279 (17)	0.6167 (11)	0.4820 (11)	0.043
C(19)	0.1525 (17)	0.6943 (11)	0.4597 (11)	0.058
C(20)	0.1764 (15)	0.5552 (10)	0.5304 (10)	0.035
C(21)	0.0941 (16)	0.5824 (11)	0.5845 (11)	0.053
C(22)	0.0540 (17)	0.5286 (11)	0.6412 (12)	0.053
C(23)	0.0876 (16)	0.4482 (11)	0.6455 (11)	0.041
C(24)	0.1609 (15)	0.4180 (11)	0.5885 (11)	0.045
C(25)	0.2066 (15)	0.4705 (10)	0.5318 (11)	0.034
C(26)	0.2588 (17)	0.3655 (11)	0.4418 (11)	0.040
C(27)	0.1877 (25)	0.5565 (16)	0.2316 (18)	0.130
N(5)	0.1460 (16)	0.5272 (11)	0.1488 (2)	0.083
C(28)	0.0674 (22)	0.4577 (14)	0.1293 (14)	0.095
C(29)	0.1765 (24)	0.5642 (17)	0.0817 (16)	0.115
O3	0.2487 (17)	0.6283 (12)	0.0944 (12)	0.141

^{a} Equivalent isotropic temperature factor U_{eq} defined as one-third of the trace of the orthogonal U_{ij} tensor for all.
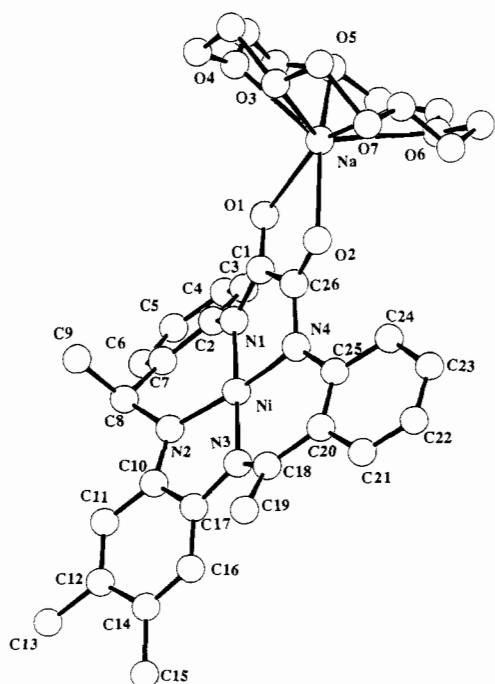

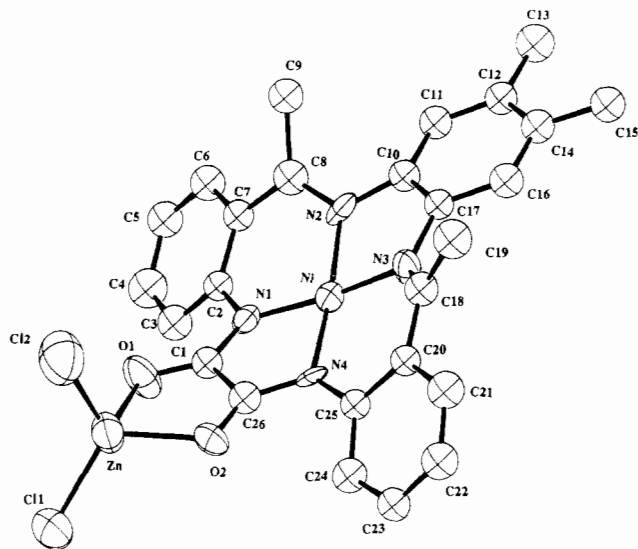**Figure 4.** Structure of [(5-crown-15)Na][Ni(α-diketo-TAD-Me$_4$+H)] as drawn by ORTEP with isotropic thermal ellipsoids.

Figure 5. Structure of the [Ni(α-diketo-TAD-Me$_4$)]ZnCl$_2$ as drawn by ORTEP with thermal ellipsoids drawn at the 50% probability level.

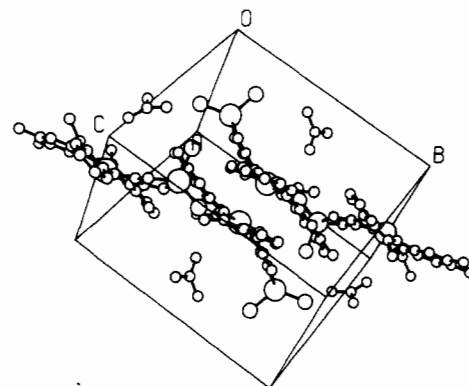**Figure 6.** PLUTO^{47} packing diagram of [Ni(α-diketo-TAD-Me$_4$)]-ZnCl$_2$·DMF.

stituted; however, they adopt saddle-shaped conformations when they are methyl substituted[31] in positions proximal to the phenyl rings. The methyl groups apparently interact sterically with the phenyl rings and cause the phenyl rings and the diiminato chelate rings to tilt on opposite sides of the N$_4$ coordination plane. Similarly, saddle-shaped conformations are found with [16]N$_4$ macrocyclic complexes[32] and have been attributed to "strained" Ni–N bonds.[33]

Other than the somewhat short Ni–Ni distance observed in the crystal structure of IVa, a short Ni–Ni distance of 3.16 Å is observed in the structure of VII. The molecules in VII do not stack as in IVa, but rather they occur in pairs that can be described as loosely held dimers (Figure 6). The Ni atoms in IVa are equally spaced along the stacking direction by 4.059 (1) Å. This distance is longer than the corresponding Ni–Ni distances in the stacked compounds Ni(dpg)$_2$^{34} (3.547 Å) and Ni(dmg)$_2$^{34} (3.25 Å) and shorter than the Ni–Ni distance in NiPc,^{34} where Pc = phthalocyanine (4.79 Å). Partially oxidized[34] stacked nickel glyoximes and phthalocyanines have shorter Ni–Ni distances, usually around 3.1 Å.

In all structures the metal is in the macrocycle cavity in a square-planar environment. The Ni atom is very nearly coplanar with the N$_4$ planes in IVa and VI. In VII the Ni atom is located above (0.13 Å) and the Zn atom below (1.8 Å) the N$_4$ plane. In

(32) Hawkinson, S. W.; Fleischer, E. B. *Inorg. Chem.* **1969**, *8*, 2402–2410.
(33) *Coordination Chemistry of Macrocyclic Compounds*; Melson, G. A., Ed.; Plennum Press: New York, 1979.
(34) Cowie, M.; Gleizes, A.; Grynkewich, G. W.; Kalina, D. W.; McClure, M. S.; Scarine, R. P.; Teitelbaum, R. C.; Ruby, S. L.; Ibers, J. A.; Kannewurf, C. R.; Marks, T. J. *J. Am. Chem. Soc.* **1979**, *101*, 2921–2934.

Table VI. Selected Bond Lengths (Å) and Angles (deg) for Ni(α-diketo-TAD-Me$_4$) (IVa), Et$_4$N[Ni(α-diketo-TAD-Me$_4$+H)]·0.8C$_6$H$_{12}$O$_2$ (V), [(5-crown-15)Na][Ni(α-diketo-TAD-Me$_4$+H)] (VI), and [Ni(α-diketo-TAD-Me$_4$)]ZnCl$_2$·HCON(Me)$_2$ (VII)

Distances

	IVa	V	VI	VII		IVa	V	VI	VII
Ni–N(1)	1.846 (4)	1.858 (8)	1.882 (10)	1.865 (14)	Na–O(1)			2.469 (10)	
Ni–N(2)	1.874 (4)	1.830 (7)	1.845 (11)	1.893 (13)	Na–O(2)			2.310 (10)	
Ni–N(3)		1.876 (7)	1.899 (10)	1.881 (14)	Zn–O(1)				2.034 (11)
Ni–N(4)		1.863 (7)	1.870 (10)	1.852 (13)	Zn–O(2)				2.023 (11)
N(1)–C(1)	1.358 (6)	1.342 (11)	1.32 (2)	1.31 (2)	Zn–Cl(1)				2.163 (6)
N(1)–C(2)	1.394 (6)	1.419 (11)	1.43 (1)	1.44 (2)	Zn–Cl(2)				2.181 (7)
N(2)–C(8)	1.318 (6)	1.455 (11)	1.47 (2)	1.31 (2)	Ni–Ni	4.059 (1)			3.165 (3)
N(2)–C(10)	1.430 (6)	1.345 (11)	1.33 (2)	1.40 (2)	Ni–Na			5.070 (9)	
N(3)–C(17)		1.422 (11)	1.40 (2)	1.43 (2)	Ni–Zn				5.140 (3)
N(3)–C(18)		1.318 (10)	1.33 (1)	1.33 (2)	C(2)–C(3)	1.410 (7)	1.37 (1)	1.36 (2)	1.38 (2)
N(4)–C(25)		1.408 (11)	1.42 (1)	1.42 (2)	C(3)–C(4)	1.387 (8)	1.37 (1)	1.39 (2)	1.41 (2)
N(4)–C(26)		1.351 (11)	1.34 (2)	1.34 (2)	C(4)–C(5)	1.364 (9)	1.40 (2)	1.35 (2)	1.35 (2)
C(8)–C(9)	1.505 (7)	1.54 (1)	1.55 (2)	1.54 (2)	C(5)–C(6)	1.377 (9)	1.38 (1)	1.39 (2)	1.36 (2)
C(8)–C(7)	1.453 (7)	1.51 (1)	1.51 (2)	1.45 (2)	C(6)–C(7)	1.418 (7)	1.41 (1)	1.40 (2)	1.39 (2)
C(2)–C(7)	1.418 (7)	1.41 (1)	1.40 (2)	1.40 (2)	C(10)–C(11)	1.386 (6)	1.44 (1)	1.40 (2)	1.39 (2)
C(10)–C(10')	1.393 (9)				C(11)–C(12)	1.375 (7)	1.37 (1)	1.37 (2)	1.37 (2)
C(10)–C(17)		1.42 (1)	1.43 (2)	1.38 (2)	C(12)–C(12')	1.412 (11)			
C(18)–C(19)		1.51 (1)	1.51 (2)	1.53 (2)	C(12)–C(14)		1.43 (1)	1.42 (2)	1.38 (2)
C(18)–C(20)		1.48 (1)	1.43 (2)	1.43 (2)	C(12')–C(11')	1.375 (7)			
C(20)–C(25)		1.42 (1)	1.38 (2)	1.41 (2)	C(14)–C(16)		1.38 (1)	1.35 (2)	1.41 (2)
C(1)–C(1')	1.563 (6)				C(11)–C(10')	1.386 (6)			
C(1)–C(26)		1.53 (1)	1.51 (2)	1.54 (2)	C(16)–C(17)		1.37 (1)	1.38 (2)	1.40 (2)
C(1)–O(1)	1.214 (6)	1.251 (11)	1.24 (1)	1.28 (2)	C(20)–C(21)		1.41 (1)	1.42 (2)	1.42 (2)
C(26)–O(2)		1.231 (10)	1.23 (1)	1.23 (2)	C(21)–C(22)		1.37 (1)	1.35 (2)	1.38 (2)
O(1)–O(1')	2.723 (8)				C(22)–C(23)		1.38 (1)	1.35 (2)	1.35 (2)
O(1)–O(2)		2.729 (9)	2.720 (12)	2.66 (2)	C(23)–C(24)		1.37 (1)	1.41 (2)	1.40 (2)
					C(24)–C(25)		1.42 (1)	1.40 (2)	1.40 (2)

Angles

	IVa	V	VI	VII		IVa	V	VI	VII
N(1)–Ni–N(2)	93.4 (2)	92.7 (4)	93.5 (5)	93.6 (6)	C(25)–N(4)–Ni		123.8 (7)	124.7 (8)	127 (1)
N(1)–Ni–N(4)		86.1 (3)	84.4 (4)	85.4 (6)	C(26)–N(4)–Ni		115.3 (7)	113.6 (9)	114 (1)
N(2)–Ni–N(3)		86.1 (3)	85.4 (5)	85.6 (6)	C(25)–N(4)–C(26)		120.9 (8)	121 (1)	118 (2)
N(3)–Ni–N(4)		97.0 (4)	96.8 (4)	94.3 (6)	C(7)–C(8)–N(2)	120.6 (4)	110.3 (8)	109 (1)	123 (2)
N(1)–Ni–N(1')	87.2 (2)				C(7)–C(8)–C(9)	119.3 (4)	111.4 (9)	111 (1)	115 (2)
N(2)–Ni–N(2')	86.0 (2)				C(9)–C(8)–N(2)	120.1 (4)	110.9 (8)	112 (1)	122 (2)
C(1)–N(1)–Ni	111.0 (3)	113.8 (7)	114.4 (9)	113 (1)	C(20)–C(18)–N(3)		120.1 (9)	122 (1)	121 (2)
C(2)–N(1)–Ni	125.9 (3)	126.9 (7)	124.6 (9)	127 (1)	C(19)–C(18)–N(3)		123.6 (8)	121 (1)	123 (2)
C(1)–N(1)–C(2)	123.0 (4)	118.9 (9)	121.0 (12)	119 (1)	C(19)–C(18)–C(20)		116.2 (8)	118 (1)	117 (2)
C(8)–N(2)–Ni	126.3 (3)	124.1 (6)	125.8 (9)	124 (1)	O(1)–Na–O(2)			69.3 (3)	
C(10)–N(2)–Ni	109.2 (3)	113.8 (6)	114.7 (9)	111 (1)	O(1)–Zn–O(2)				81.8 (5)
C(8)–N(2)–C(10)	124.2 (4)	120.3 (8)	118 (1)	123 (2)	O(2)–Zn–Cl(2)				108.3 (4)
C(17)–N(3)–Ni		112.6 (6)	112.1 (8)	112 (1)	O(1)–Zn–Cl(1)				112.7 (4)
C(18)–N(3)–Ni		121.8 (6)	123.2 (9)	126 (1)	Cl(1)–Zn–Cl(2)				120.6 (2)
C(17)–N(3)–C(18)		123.3 (8)	123 (1)	120 (1)					

(a)   (b)   (c)   (d)
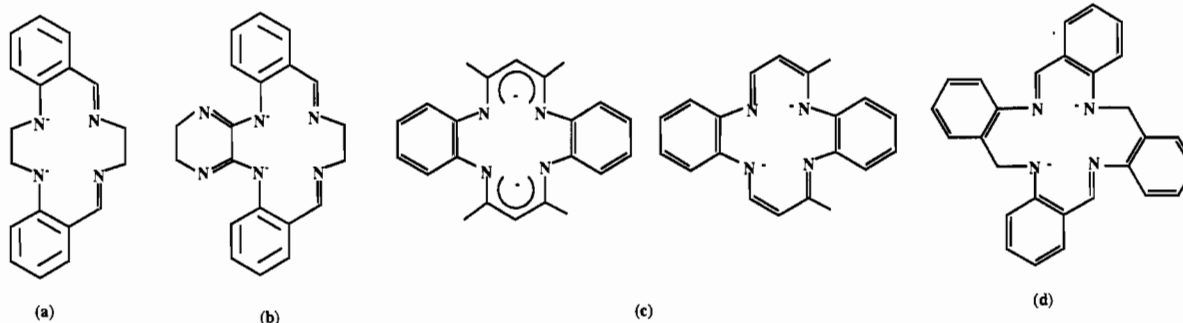
Figure 7. Related macrocycles with saddle-shaped structures.

this configuration the Zn atom is located 5.140 (3) Å from the Ni atom. This distance is slightly longer than the corresponding Na–Ni distance in VI, which is found at 5.070 (9) Å.

The Ni–N distances in all structures are similar, with a mean value of 1.865 (8) Å. There is no significant increase in this distance in any of the reduced materials (V, VI) that may be attributed to the saturation of one of the imino bonds. This value is in good agreement with the Ni–N distances observed in highly conjugated systems with trigonal nitrogen atoms. In closely related structures[30] (Figure 7a,b) the mean Ni–N distance is 1.85 Å.[30] There are no intermolecular Ni–N or Ni–O interactions in any

of the structures reported herein, and the Ni atoms are four-coordinate. The four-coordinate, planar geometry is maintained in solution, as indicated by the nearly identical electronic spectra in both coordinating and noncoordinating solvents. Similarly, the expected diamagnetism of these low-spin d^8 complexes is apparent in the NMR spectra and magnetic measurements (vide infra). In general, no differences are observed among the analogous bonds and angles in all four structures (Table VI). The only exception is found in the N(2)–C(8) distances, which are elongated by 0.1 Å and the N(2)–C(10) distances, which are contracted by the same amount in the reduced complexes (V, VI). Similarly, the

Table VII. Electrochemistry of the Complexes[a]

compd	solvent[b]	E_{pc}, V	$|E_{pc} - E_{pa}|$, mV	i_{pa}/i_{pc}	conc, mM	$i_{pc}/V^{1/2}C$	$E_{1/2}$, V[c]
Ni(α-diketo-TAD-Me$_4$)	acetone	-1.272	71	1.09	1.0	52	-1.236
	CH$_2$Cl$_2$	-1.275	117[d]	0.97	1.7	8[e]	-1.216
	DMF	-1.256	73	0.91	1.0	41	-1.220
Ni(α-diketo-TAD-Me$_2$)	DMF	-1.201	79	1.07	0.97	39	-1.161
Ni(α-diketo-TAD-Me$_2$)	DMF	-1.207 (irr)			1.2		
Ni(α-diketo-TAD)	DMF	-1.156 (irr)			1.03		
Et$_4$N[Ni(α-diketo-TAD-Me$_4$+H)]	DMF	+0.073 (irr)					
Co(α-diketo-TAD-Me$_2$)	DMF	-0.919	104	0.98	2.44	10[e]	-0.866
Co(ethylene-TAD-Me$_2$)	DMF	-1.512	73	0.96	3.77	6[e]	-1.480

[a] Solutions were 0.1 M in *n*-Bu$_4$NClO$_4$. Potentials are reported versus the saturated calomel electrode. [b] At Pt working electrode. [c] $E_{1/2}$ values were taken as the average of E_{pc} and E_{pa} values. [d] iR drop in CH$_2$Cl$_2$ was not compensated. [e] A smaller Pt-bead working electrode was used in the cyclic voltammetry of this complex in CH$_2$Cl$_2$ as well as in the cyclic voltammetry of the Co^{II} complex. Both electrodes were calibrated by using (Et$_4$N$^+$)$_2$Ni(MNT)$_2$ as a standard. The current function for the standard was 10 in both CH$_2$Cl$_2$ and DMF for the smaller electrode, and for the bigger electrode it was 62 in acetone and 55 in DMF.

angles around C(8) are affected, as hybridization changes from sp^2 to sp^3 upon reduction. In compounds IVa and VII, the mean value for C(7)–C(8)–N(2), C(7)–C(8)–C(9), and C(9)–C(8)–N(2) is 120°; in the reduced complexes V and VI this value is reduced to 111°. The N(1)–C(1) and N(4)–C(26) distances with a mean value of 1.34 (2) Å for all structures are comparable with the corresponding distances in a similar macrocycle (Figure 7b)[30] but are significantly shorter than those in another (Figure 7a). The shortening of these bonds has been attributed earlier[30] to an extension of the conjugated system through them.

In all structures the double-bond character of the α-diketone carbonyls is pronounced as evidenced by the short C–O bonds. These are not affected by reduction (V, VI) and may be slightly elongated by coordination of ZnCl$_2$ in VII. The C–O distances of the 6,11-dimethyl-7,10-diazahexadeca-5,11-diene-2,4,13,15-tetraone ligand[35] are 1.245 Å.

In VII the zinc atom is four-coordinate, in a distorted tetrahedral environment, bonded by the α-diketo portion of the macrocycle and the two chloride ligands. Although one DMF solvent molecule per macrocycle is present in the structure, the DMF is not a ligand for zinc, but rather fulfills packing requirements of the lattice (Figure 6). The Zn–Cl bond length, at 2.172 (6) Å, is similar to that determined for other Zn–Cl (terminal) bonds, in mononuclear,[36] dinuclear,[37] heterobinuclear,[38] and cluster[39] complexes, with tetrahedrally coordinated zinc atoms. The Zn–O bond lengths are similar to those determined for acacen[40] and acac[41] complexes or complexes of bidentate bridging carboxylates.[42]

In compound VI the sodium cation is coordinated by the α-diketo portion of the macrocyclic ligand and the crown ether molecule. The Na–O bonds involving the carbonyl oxygens of the ligand (mean value 2.37 (1) Å) compare with those in Na-salen,[12] Na-acacen,[12d] and [(Co(salen)Na]$_2$(dicyclohexano-18-crown).[12a] The high thermal parameters (and standard deviations) observed for the crown ether molecule in VI are due to positional disorder. The crown ether molecule in VI was best refined with

three components with occupancies 0.5, 0.3, and 0.2 at their respective sites, and the intramolecular distances within the crown were fixed. The Na–O bonds were found within a range 2.31 (1)–2.75 (5) Å.

Cyclic Voltammetry. Table VII summarizes electrochemical results obtained in various solvents for the complexes. The ZnCl$_2$ and Cu(nNO$_3$)$_2$ adducts of IVa are insoluble in nonpolar, noncoordinating solvents and in DMF undergo solvolysis. As a result, their electrochemical behavior could not be established. The cyclic voltammetry of the Ni^{II} complex (IVa) was not appreciably different in polar, nonpolar, or protic solvents at potentials <0 V. In acetone, a reversible reduction was observed at a high negative potential, $E_{1/2}$ = -1.236 V vs SCE. No other oxidations or reductions were observed in the useful range of this solvent, ~+1.0 to -1.5 V. The same reduction wave was observed at $E_{1/2}$ = -1.216 vs SCE in CH$_2$Cl$_2$, where two irreversible oxidations at high positive potentials E_{pa_1} = +1.236 V and E_{pa_2} = +1.344 V vs SCE also were observed. In DMF, there is a reduction wave at $E_{1/2}$ = -1.220 V. The process is reversible at high scan rates and becomes quasireversible at low scan rates with i_{pa}/i_{pc} = 0.89 at 100 mV/s and i_{pa}/i_{pc} = +0.82 at 50 mV/s. Also, a quasireversible oxidation is observed in the same solvent, with $E_{1/2}$ = +0.878 V vs SCE. Similar electrochemical behavior is exhibited by the complex IVb (Scheme II), which is not methyl substituted on the phenylenediamine portion. The reversible reduction occurs at $E_{1/2}$ = -1.161 V vs SCE, and there is an irreversible oxidation at E_{pa} = +0.846 V vs SCE. In complexes IVc and IVd, the reduction wave becomes totally irreversible at E_{pc} = -1.207 V and E_{pc} = -1.156 V vs SCE, respectively. It appears that methyl substitution on the imine carbon stabilizes the species IV$^-$. The cyclic voltammetry of the reduced product obtained by the reaction of IVa with Et$_4$NBH$_4$ in acetone shows an irreversible oxidation (E_{pa} = +0.073 V). The quasireversible Co^{II}/Co^I reduction for the Co^{II} analogue of IVc is observed at $E_{1/2}$ = -0.866 V. An irreversible oxidation also is observed at E_{pa} = +0.184 V. Bubbling of oxygen gas in the electrochemistry cell for 5 min causes complete disappearance of the reduction wave. A new, irreversible wave appears at E_{pc} = -1.127 V, and the electronic spectrum of the oxygenated solution shows an absorption at 470 nm. This spectrum is different than that of the Co^{II}(α-diketo-TAD-Me$_4$) complex, which shows a shoulder at 530 nm. Bubbling of argon gas in the electrochemistry cell for another 5 min causes disappearance of the irreversible wave, reestablishes the original reduction at $E_{1/2}$ = -0.866 V, and brings back an electronic spectrum identical with that of Co^{II}(α-diketo-TAD-Me$_4$). A solution of the latter when exposed to air, slowly changes color as the absorption at 530 nm loses intensity and a new absorption emerges as a shoulder at 470 nm. The change is complete over a period of a few hours. We believe that the species which forms upon exposure to air is the same as the one obtained during the cyclic voltammetry experiment and is due to the formation of a dioxygen adduct. The same cyclic voltammetry experiment was repeated for the complexes Co^{II}(ethylene-TAD-Me$_2$), and Co^{II}[ethylene-TAD-(OMe)$_2$], which are analogues of Co^{II}(α-diketo-TAD-Me$_2$) but lack the α-diketone functionality.[43] Both species have clean

(35) Bailey, N. A.; Fenton, D. E.; Gayda, S. E.; Phillips, C. A. *J. Chem. Soc., Dalton Trans.* **1984**, 2289–2292.
(36) (a) Mak, T. C. W.; Huang, S. H. *Polyhedron* **1987**, *6*, 1111–1114. (b) Ball, R. G.; Brown, R. S.; Cocho, J. L. *Inorg. Chem.* **1984**, *23*, 2315–2318. (c) Kosky, C. A.; Gayda, J. P.; Gibson, J. F.; Jones, S. F.; Williams, D. J. *Ibid.* **1982**, *21*, 3173–3179. (d) Nicholson, G. A.; Petersen, J. L.; McCormick B. J. *Ibid.* **1982**, *21*, 3274–3280.
(37) (a) Cotton, F. A.; Duraj, S. A.; Extine, M. W.; Lewis, G. E.; Roth, W.; Schmulbach, C. D.; Schwotzer, W. *J. Chem. Soc., Chem. Commun.* **1983**, 1377–1378. (b) Coucouvanis, D.; Greiwe, K.; Salifoglou, A.; Challen, P.; Simopoulos, A.; Kostikas, A. *Inorg. Chem.* **1988**, *27*, 593–594.
(38) Cotton, F. A.; Duraj, S. A.; Roth, W.; Schmulbach, C. D. *Inorg. Chem.* **1985**, *24*, 525–527.
(39) Dance, I. G. *Inorg. Chem.* **1981**, *20*, 2155–2160.
(40) Glick, M. D.; Lintvedt, R. L. *Inorg. Chem.* **1976**, *15*, 1654–1660.
(41) Belford, R. L.; Chasteen, N. D.; Hitchman, M. A.; Hon, P. K.; Pflunger, C. E.; Paul, I. C. *Inorg. Chem.* **1969**, *8*, 1312–1319.
(42) (a) Clegg, W.; Little, I. R.; Straughan, B. P. *J. Chem. Soc., Dalton Trans.* **1986**, 1283–1288. (b) Cotton, F. A.; Duraj, S. A.; Roth, W. *Inorg. Chem.* **1984**, *23*, 4042–4045. (c) Clegg, W.; Little, I. R.; Straughan, B. P. *Inorg. Chem.* **1988**, *27*, 1916–1923.

Table VIII. Electronic Spectral Data for the Complexes and the Free Ligand

compd	solvent	λ_{max}, nm	ϵ, M^{-1} cm^{-1}
Ni(α-diketo-TAD-Me$_4$)	DMF	518	1150
		394	9940
		310 (sh)	
		282 (sh)	
Et$_4$N[Ni(α-diketo-TAD-Me$_4$+H)]	DMF	710	2138
		536	3594
		439	6620
[(5-crown-15)Na][Ni(α-diketo-TAD-Me$_4$+H)]	DMF	710	2840
		536	3690
		439	5676
Co(α-diketo-TAD-Me$_2$)	DMF	530 (sh)	
		310	23600
free ligand (α-diketo-TAD-Me$_2$)	DMF	394 (sh)	
		328	22576
		274 (sh)	
Ni(α-diketo-TAD-Me$_4$)ZnCl$_2$[a]	DMF	570	1182

[a] This compound is insoluble in nonpolar solvents and dissolves in DMF with dissociation of ZnCl$_2$; the visible spectrum was obtained in 0.1 M ZnCl$_2$ solution, with 1 mM initial concentration of the complex.

electrochemistry in DMF, with reversible reduction waves at $E_{1/2}$ = −1.480 V and $E_{1/2}$ = −1.520 V, respectively, and quasireversible oxidation waves at $E_{1/2}$ = +0.205 V and $E_{1/2}$ = +0.138 V. Bubbling of oxygen gas for a brief period of time (up to 15 min) does not generate cleanly a new electroactive species, and no changes in the color of the solutions are evident. It appears that the electron-withdrawing oxalyl group (α-diketone functionality) dramatically raises the reduction potential in the Co-containing IVc complex and possibly allows for the reversible facile addition of dioxygen. An additional consequence of the electron-withdrawing effects of the oxalyl group is an apparent weakening of the ligand field around the Co^{II} ion in Co^{II}(α-diketo-TAD-Me$_4$) that results in a high-spin complex (vide infra). It should be noted that Co^{II}(ethylene-TAD-Me$_2$) and Co^{II}[ethylene-TAD-(OMe)$_2$] without the α-diketone group[43] are low spin with ESR spectra typical for Co^{II} square-planar macrocyclic complexes.

Electronic Spectra. The electronic spectra of the complexes are shown in Table VIII. The electronic spectra of Schiff-base macrocycles with extended π-conjugated chromophores exhibit intense transitions in the visible region, which mask the Ni^{II} d → d bands.[33] In all of the complexes reported in this paper, the absorptions observed in the visible region between 750 and 400 nm exhibit high extinction coefficients and arise mainly from M → L or L → M CT processes. In the free ligand (III), the band at 328 nm with ϵ = 22576 M^{-1} cm^{-1} is assigned to a ligand π → π^* transition. In the Co^{II} macrocyclic complex this absorption appears hypsochromically shifted at 310 nm with a similar extinction coefficient. The same absorption also is present in the Ni^{II} macrocycle and appears as a shoulder at 310 nm. The reduction products obtained either by Et$_4$NBH$_4$ reduction or Na amalgam reduction possess the same chromophore and therefore exhibit very similar visible spectra. It was difficult to obtain

information on the visible spectra of the adducts, because of the dissociation occuring in solvents where they dissolve; however, the visible spectrum of the Zn adduct, obtained in the presence of excess ZnCl$_2$ in a DMF solution, showed an absorption band at 570 nm. This band is bathochromically shifted relative to the corresponding band in IVa that occurs at 518 nm. Such a bathochromic shift would be consistent with an assignment of the 518-nm absorption as a M → Lπ^* transition.

Magnetic Properties and NMR Spectra. The Ni^{II}(α-diketo-TAD-Me$_4$) complex is a square-planar, diamagnetic complex. The sharp, unshifted ^{1}H NMR spectra of Ni^{II}(α-diketo-TAD-Me$_4$), V, and VI also indicate the diamagnetic nature of these complexes in solution. In the spectra of V and VI a new resonance appears as a quartet and is assigned to the proton added on the imine bond.

The magnetic moment of the Cu(NO$_3$)$_2$ adduct measured on a solid microcrystalline sample was 1.87 μ_B. The magnetic moment μ^{corr}_{eff} of the crystalline Co^{II} complex measured at 150 K on a SQUID magnetometer was found to be 4.23 μ_B and revealed an unusual case of high-spin Co^{II}N$_4$ macrocycle. The X-ray crystal structure of this complex shows the Co^{II} ion four-coordinate and planar.[44] The reduction of the ligand field, sufficient to cause an unpairing of electrons, must be attributed to the electron-withdrawing effects of the α-diketo group. A study of the electronic structures of square-planar complexes of Co^{II} with some N$_4$ macrocyclic ligands has been reported by Nishida and co-workers.[45] In this study it was concluded that in Co^{II}[14]N$_4$ macrocycles very similar to IV, the d$_{xz}$ and d$_{yz}$ orbitals suffer remarkable antibonding effects as a consequence of interactions with π orbitals of the ligands. Such effects, in extreme cases, can in fact lead to a spin crossover from a low-spin ($S = ^1/_2$) to a high-spin ($S = ^3/_2$) ground state.

(43) The ligand 2,3-ethylene-5,6,13,14-dibenzo-9,10-(4',5'-dimethylbenzo)-1,4,8,11-tetraazacyclotetradeca-7,12-diene is abbreviated as ethylene-TAD-Me$_2$, and the 4',5'-dimethoxy derivative, as ethylene-TAD-(OMe)$_2$: Coucouvanis, D.; Christodoulou, D. Manuscript in preparation.

(44) Poor quality of the crystals did not allow accurate determination of bond distances and angles for Co(α-diketo-TAD-Me$_2$). Crystal and refinement data for Co(α-diketo-TAD-Me$_2$): a = 6.877 (1) Å, b = 11.945 (10) Å, c = 23.062 (9) Å, $\alpha = \beta = \gamma = 90.0°$, space group $P2_12_12_1$, d_{calcd} = 1.59 g/cm^3, d_{obsd} = 1.56 g/cm^3, μ = 9.0 cm^{-1}, $2\theta_{max}$ = 40° (λ(Mo Kα) = 0.71069 Å), 3773 unique reflections, 2276 reflections used in refinement ($F_o^2 > 3\sigma(F_o^2)$), 141 variable parameters, final R = 0.012.

(45) (a) Nishida, Y.; Hayashida, K.; Sumida, A.; Kida, S. *Inorg. Chim. Acta* **1978**, *31*, 19–23. (b) Nishida, Y.; Hayashida, K.; Naoyasu, O.; Kida, S. *Inorg. Chim. Acta* **1980**, *38*, 213–219.

(46) Johnson, C. K. Report ORNL-3794; Oak Ridge National Laboratory: Oak Ridge, TN, 1965.

(47) PLUTO78 package, Cambridge, U.K.